Inhibition by 4-aminopyridine of HERG K^+ channels expressed in a mammalian cell line

John M. Ridley, James T. Milnes, Harry J. Witchel and Jules C. Hancox

Department of Physiology and Cardiovascular Research Laboratories, School of Medical Sciences, University Walk, Bristol BS8 1TD, UK

4-Aminopyridine (4-AP) is used extensively in the field of cardiac muscle electrophysiology to study the role(s) in cardiac tissue of transient outward K^+ current (I_{to}). Although millimolar 4-AP is widely considered to be selective for I_{to}, results of a previous study from this laboratory suggested that 4-AP might, in addition, exert an inhibitory effect on the rapid delayed rectifier K^+ current, I_{Kr} (Mitcheson & Hancox, 1999). The aim of the present study was to investigate further this possibility, by characterising effects of 4-AP on heterologously expressed HERG channels, since *HERG* (*human-ether-a-go-go*-related gene) encodes the pore-forming subunit of channels responsible for I_{Kr} (Sanguinetti & Keating, 1997).

Measurements of whole-cell HERG current (I_{HERG}) were made at 37 ± 1 °C from a mammalian cell line (HEK-293) stably expressing HERG (Zhou *et al.* 1998). I_{HERG} 'tail' amplitude was monitored at −40 mV, following activating pulses to +30 mV. 4-AP was found to exert a concentration-dependent inhibitory effect on I_{HERG}, with a half-maximal inhibitory concentration (IC_{50}) of 4.4 ± 0.5 mM (mean ± S.E.M.; n = minimum of 5 cells for each of seven 4-AP concentrations between 0.1 and 100 mM). Positive control experiments under similar conditions with the methanesulphonanilide HERG blocker E-4031 gave an IC_{50} value near to 12 nM, which is close to an IC_{50} value (7.7 nM) observed previously for E-4031 with this cell line (Zhou *et al.* 1998). Inhibition of I_{HERG} by 5 mM 4-AP was observed to be voltage dependent; 4-AP also shifted voltage-dependent activation of I_{HERG} towards more negative voltages, producing a mean shift in half-maximal activation of −7.4 ± 0.9 mV (n = 8 cells). In experiments utilising a ventricular AP waveform as the voltage command, 5 mM 4-AP suppressed the peak outward I_{HERG} elicited during the AP repolarisation phase by 58.5 ± 4.1 % (n = 5 cells).

We conclude that 4-AP is a low-affinity blocker of cardiac HERG potassium channels, blocking I_{HERG} with a potency similar to that suggested for I_{Kr} from previous experiments on rabbit native cardiomyocytes (Mitcheson & Hancox, 1999). Since 4-AP concentrations in the millimolar range are used in investigations of cardiac I_{to}, our results confirm that an accessory inhibitory effect on I_{Kr} may need to be taken into account in interpreting data that might otherwise be ascribed to selective inhibition of I_{to}.

Mitcheson, J.S. & Hancox, J.C. (1999). *Pflügers Arch.* **438**, 68–78.

Sanguinetti, M.C. & Keating, M.T (1997). *NIPS* **12**, 152–157.

Zhou, Z. *et al.* (1998). *Biophys. J.* **74**, 230–241.

This work was supported by the British Heart Foundation and The Wellcome Trust.

A Ca^{2+}-activated non-selective cation channel expressed in human atrial cardiomyocytes

R. Guinamard, A. Chatelier, P. Corbi, M. Rahmati, J. Lenfant and P. Bois

UMR 6558, LBSC, Université de Poitiers, 86022 Poitiers cedex, France

$[Ca^{2+}]$ overload leads to cardiac arrhythmias induced by delayed afterdepolarisations, and has been attributed to a transient inward current (I_{ti}). This current appears to be the result of Na^{2+}–Ca^{2+} exchange, a Ca^{2+}-activated chloride current and a Ca^{2+}-activated non-selective cationic current (Ehara *et al.* 1988). Using the cell-free configuration of the patch-clamp technique, we have characterized the electrophysiological properties of a Ca^{2+}-activated non-selective cation channel (NSC_{Ca}) on freshly dissociated human atrial cardiomyocytes.

Myocardium specimens were obtained from patients undergoing cardiac surgery according to the European Community Council Directive. All patients had normal sinusal rhythmicity. Cells were obtained by both enzymatic and mechanical dissociation. Before patching, cells were incubated for at least 10 min with 500 nM phorbol 12-myristate, 13-acetate (PMA), a PKC activator. Channel currents were recorded in inside-out patches bathed on both sides with a solution containing (mM): 140 NaCl, 4.8 KCl, 1.2 $MgCl_2$, 1 $CaCl_2$, 10 glucose and 10 Hepes. In these conditions, the channel had a linear current–voltage relationship (γ = 19 ± 0.4 pS, mean ± S.E.M., n = 7). Depolarisation increased channel open probability. Ion substitution experiments indicated that the channel discriminated poorly among monovalent cations (P_K/P_{Na} = 1.17 ± 0.08, n = 6), and was impermeable to Cl^- (P_{Cl}/P_{Na} = 0.1 ± 0.04, n = 6) and Ca^{2+} (P_{Ca}/P_{Na} = 0.13 ± 0.03, n = 3). Possible regulatory properties of the channel were investigated; channel openings were seen at 1 mM $[Ca^{2+}]_i$ but not at 1 nM (n = 6). The channel activity was reduced to about 50 % of the control (n = 3) by the intracellular application of 1 mM ATP.

As a rise in $[Ca^{2+}]$ increases channel activity, we conclude that the NSC_{Ca} channel is a good candidate to support, at least in part, delayed afterdepolarisations observed in $[Ca^{2+}]$ overload and thus could be implicated in arrhythmia generation. Interestingly, we previously showed that a similar channel was present on dedifferentiated rat cardiomyocytes in culture, a model of cardiac hypertrophy that leads to arrhythmia (Guinamard *et al.* 2002).

Ehara, R. *et al.* (1988). *J. Physiol.* **403**, 117–133.

Guinamard, R. *et al.* (2002). *J. Memb. Biol.* **188**, 127–135.

All procedures accord with the Declaration of Helsinki.

Slowed inactivation of the sodium current (I_{Na}) in isolated ventricular myocytes from hypertrophied guinea-pig heart

A. Chorvatova, R.L. Snowdon, G. Hart and M. Hussain

Department of Medicine, University of Liverpool, Liverpool L69 3GA, UK

Prolongation of the action potential is a characteristic feature of cardiac hypertrophy. However, the ionic currents underlying the longer action potential are not fully described. We therefore investigated the role of I_{Na} in prolongation of the action potential in a mild model of hypertrophy in the guinea-pig.

Hypertrophy was produced by pressure overload caused by constriction of the abdominal aorta with a silver clip (i.d.

0.5 mm). Age- and weight-matched cohorts underwent the same procedure (sham) except the aorta was not clipped (Bryant *et al.* 1997). After 20 weeks, guinea-pigs were anaesthetised with sodium pentabarbitone (200 mg kg^{-1}, I.P.) and killed by exsanguination. Left ventricular myocytes were isolated by enzymatic digestion and voltage clamped using conventional whole-cell patch clamp. I_{Na} were recorded using large tipped microelectrodes (0.5 MΩ) and with low external [Na^+]. External solutions contained (mmol l^{-1}): NaCl, 5–20; TEACl, 120; $MgCl_2.6H_2O$, 1; $CaCl_2$, 2; glucose, 10; Hepes, 10; adjusted to pH 7.3 with TEAOH. Internal solutions contained (mmol l^{-1}): CsCl, 120; TEACl, 20; $MgCl_2.6H_2O$, 5; Na_2ATP, 5; $CaCl_2$, 1; EGTA, 5; Hepes, 10; pH 7.25 with CsOH. Current–voltage (*I–V*) relationships were constructed in the absence and presence of 25 μmol l^{-1} tetrodotoxin (TTX) following step depolarisations (for 50 ms), in 5 mV increments, from a holding potential of −80 mV. Double-pulse protocols were also used to investigate steady-state activation (d) and inactivation (f) variables. Data are shown as means ± S.E.M. and were analysed with Student's t test for independent observations.

TTX-sensitive I_{Na} density (normalised for membrane capacitance) was decreased at voltages between −45 to −30 mV ($P < 0.05$). Maximal I_{Na}, recorded following depolarisation to −30 mV (peak of the *I–V* curve), was −9.65 ± 1.3 pA pF^{-1} ($n = 5$) in control myocytes and −6.2 ± 0.5 pA pF^{-1} ($n = 6$) in hypertrophied myocytes ($P < 0.05$). The d and f variables were not significantly different between control and hypertrophied myocytes. However, the time constant for the rapid component of inactivation of I_{Na} was significantly prolonged in hypertrophied myocytes at voltages between −40 and −20 mV ($P < 0.05$).

In conclusion, these data suggest that although peak I_{Na} density was decreased and steady-state d and f variables were unchanged, slower time-dependent inactivation of I_{Na} may permit increased Na^+ influx and contribute, at least in part, to prolongation of the action potential in hypertrophied cardiac myocytes.

Bryant, S.M. *et al.* (1997). *Cardiovasc. Res.* **35**, 315–323.

This work was supported by the British Heart Foundation.

All procedures accord with current UK legislation.

Role of fast sodium current, i_{Na}, in murine sino-atrial node pacemaking

M. Lei*, M.K. Lancaster†, S.A. Jones† and M.R. Boyett†

**University Laboratory of Physiology, University of Oxford, Oxford OX1 3PT and †School of Biomedical Sciences, University of Leeds, Leeds LS2 9JT, UK*

A very interesting question is what mechanisms underlie the remarkably fast murine sino-atrial node (SAN) beating rates of 350–600 beats min^{-1}. We recently reported that fast sodium current, i_{Na}, contributes to pacemaking of isolated murine SAN cells (Lei *et al.* 2002). To further elucidate the role of i_{Na} in murine SAN pacemaking, we have studied the effect of TTX, a selective i_{Na} blocker, on the electrical activities of intact murine SAN.

Hearts were excised from 20–25 g adult C57BL mice after Schedule 1 killing by cervical dislocation. After dissection of SAN and some surrounding atrial muscle, the preparation (endocardial surface up) was fixed in a tissue bath and was superfused with Tyrode solution at 35 °C at a rate of 4–5 ml min^{-1} through a heat exchanger. Extracellular potentials (ECPs) were recorded as described by Yamamoto *et al.* (1998). ECPs in and around the SAN under control conditions showed a variety of morphologies. The activation pattern was similar to that reported from rabbit SAN (Yamamoto *et al.* 1998). Spontaneously beating SAN tissue was superfused with 1–30 μM TTX. In 6 out 6 preparations, up to 5 μM TTX caused 3:1 or 2:1 sinus-atrial (SA) conduction block and 30 μM TTX caused a complete block of SA conduction. 30 μM TTX also terminated the pacemaker activity of the peripheral region and decreased pacemaker beating rate of the leading pacemaker site by 19 ± 4 % ($n = 6$, $P < 0.01$, Student's paired t test). Figure 1 shows an example of the effect of TTX on the electrical activities of the surrounding atrial muscle and the leading pacemaking site.

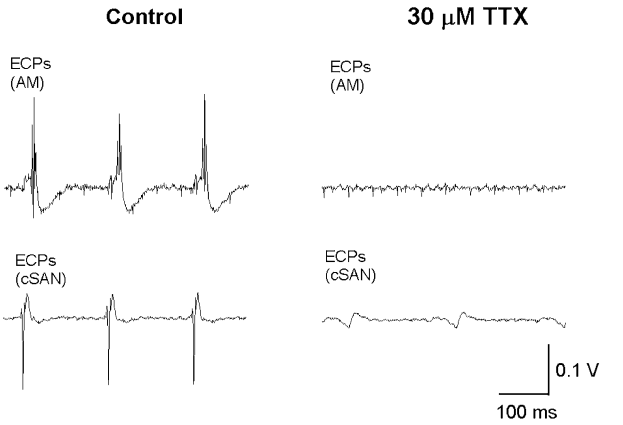

Figure 1. Extracellular potentials (ECPs) recorded from the surrounding atrial muscle (AM) and the leading pacemaker site (cSAN) in the absence (left) and presence of 30 μM TTX (right).

The results suggest that i_{Na} is of importance for maintenance of physiological pacemaking and its role is greater in the periphery than in the centre.

Lei, M. *et al.* (2002). *Biophys. J.* **82**, 605a.

Yamamoto, M. *et al.* (1998). *Cardiovasc. Res.* **39**, 360–372.

The work was supported by The Wellcome Trust.

All procedures accord with current UK legislation.

ATP-dependent effects of halothane on SR Ca^{2+} regulation in isolated saponin-permeabilized atrial myocytes from rat

Zhaokang Yang, Simon M. Harrison and Derek S. Steele

School of Biomedical Sciences, University of Leeds, Woodhouse Lane, Leeds LS2 9JT, UK

The effect of halothane on sarcoplasmic reticulum (SR) Ca^{2+} regulation was investigated in saponin-permeabilized rat atrial myocytes. Rats (250–300 g) were killed humanely (Schedule 1) and atrial myocytes were isolated by enzymatic digestion. Cells were perfused with weakly Ca^{2+}-buffered solutions approximating to the intracellular milieu, and Ca^{2+} release from the SR was detected using fluo-3. Spontaneous Ca^{2+} release from the SR occurred when the bathing [Ca^{2+}] was increased to ~250 nM. Spontaneous release occurs when the SR Ca^{2+} content reaches a 'threshold' level. As the Ca^{2+} content increases, the frequency of localised Ca^{2+} release events (Ca^{2+} sparks) rises until a propagated Ca^{2+} wave is initiated (Cheng *et al.* 1996). The increase in spark frequency may involve Ca^{2+} binding to a regulatory site within the SR lumen, which leads to an increase in the open probability of the ryanodine receptor (RyR).

In the presence of 5 mM ATP, 1 mM halothane had no apparent effect on the amplitude or frequency of spontaneous Ca^{2+} release (Fig. 1). As reported in ventricular myocytes (Yang & Steele, 2000), decreasing the cytosolic [ATP] to 0.05 mM markedly increased the amplitude of the spontaneous Ca^{2+} transients and reduced the frequency of release. These changes are believed to reflect a reduction in the open probability of the RyR, due to reduced occupancy of the adenine nucleotide-binding site. This allows the [Ca^{2+}] within the SR to reach a higher level before propagated Ca^{2+} release occurs. In the continued presence of low [ATP], introduction of 1 mM halothane induced a marked decrease in the amplitude of the spontaneous Ca^{2+} transient (36.5 ± 4.2 %, n = 6, mean ± S.E.M.) and an increase in the release frequency (61 ± 7.6 %, n = 6, mean ± S.E.M.). This effect was reversible on removal of halothane. Further experiments showed that at 5 mM ATP, > 2 mM halothane was required to influence spontaneous Ca^{2+} release. However, in the presence of 0.05 mM ATP, halothane had a significant effect at < 0.5 mM. This is within the range (0.05–0.7 mM) recorded from arterialized blood during anaesthesia (Davies *et al.* 1972).

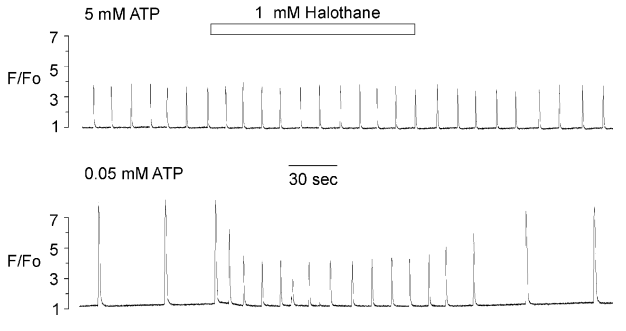

Figure 1. Effects of 1 mM halothane on spontaneous SR Ca^{2+} release in a saponin skinned atrial myocyte in the presence of 5 mM cytosolic ATP (top) and 0.05 mM ATP (bottom). The solution contained (mM): KCl, 100; Hepes, 25; EGTA, 0.05; phosphocreatine, 10; ATP, 5–0.05 and fluo-3, 0.002. The free [Ca^{2+}] and [Mg^{2+}] were 200 nM and 1 mM, respectively. pH 7.0, 22 °C.

These effects of halothane are consistent with an increase in the open probability of the RyR. The apparent ATP dependence suggests that halothane may have little direct effect on SR Ca^{2+} regulation under normal conditions. However, if cells become metabolically impaired, halothane may serve to maintain the sensitivity of the RyR as the [ATP] decreases, thereby limiting the rise in SR Ca^{2+} content. This may reduce the severity of spontaneous Ca^{2+} release during ischaemia and reperfusion.

Cheng, H. *et al.* (1996). *Am. J. Physiol.* **270**, C148–159.

Davies, D.N. *et al.* (1972). *Br. J. Anaesth.* **44**, 548–550.

Yang, Z. & Steele, D.S. (2000). *J. Physiol.* **523**, 29–44.

The financial support of the British Heart Foundation is acknowledged.

All procedures accord with current UK legislation.

Effects of halothane, isoflurane and sevoflurane on membrane currents in subepicardial and subendocardial rat left ventricular myocytes

A. Rithalia*, M.R. Boyett*, P.M. Hopkins† and S.M. Harrison*

**School of Biomedical Sciences and †Academic Unit of Anaesthesia, University of Leeds, Leeds, UK*

Halothane (HAL), isoflurane (ISO) and sevoflurane (SEVO) have a lesser abbreviating effect on action potential duration (APD) in cells isolated from the subepicardium (EPI) than the subendocardium (ENDO) of the rat left ventricle (Rithalia *et al.* 2001), suggesting differences in anaesthetic-sensitive currents in the two cell types. To investigate the mechanisms underlying the differential transmural effects of these agents on APD we measured L-type Ca^{2+} current (I_{Ca}), transient outward current (I_{to}) and steady-state current (I_{ss}) in EPI and ENDO myocytes.

Hearts were removed from humanely killed male Wistar rats (200–250 g weight) and EPI and ENDO myocytes isolated enzymatically from the left ventricle (Rithalia *et al.* 2001). Membrane currents (whole-cell patch-clamp) were recorded at 30 °C in the absence and presence of the three anaesthetics (0.6 mM and/or 1 mM) in EPI and ENDO cells (n = 7–11 cells in each group). I_{Ca} was evoked by 200 ms pulses from −40 to 0 mV and I_{to} and I_{ss} by 200 ms pulses from −80 to +80 mV (with 10 μM nifedipine to inhibit I_{Ca}). Data are presented as means ± S.E.M. P values result from paired or unpaired t tests as appropriate.

I_{Ca} was not significantly different in EPI (−0.48 ± 0.04 nA, n = 16) and ENDO (−0.50 ± 0.05 nA, n = 13) cells. HAL, ISO and SEVO (0.6 mM) significantly decreased (P < 0.005) I_{Ca} to a similar extent in EPI and ENDO cells (HAL: −30.2 ± 3.8 *vs* −24.4 ± 4.0 %; ISO: −14.5 ± 3.4 *vs* −16.7 ± 1.4 %; SEVO: −9.4 ± 1.4 *vs* −10.1 ± 1.5 %, respectively).

I_{to} was greater (P < 0.001) in EPI (3.65 ± 0.23 nA, n = 33) than ENDO (0.88 ± 0.06 nA, n = 28) cells. 0.6 mM and 1 mM HAL decreased I_{to} in EPI cells, by 8.3 ± 1.7 % (P = 0.004) and 17.9 ± 2.1 % (P = 0.002), respectively. ISO (1 mM) and SEVO (1 mM) also significantly decreased I_{to} in EPI cells (ISO: −13.2 ± 1.9 %, P = 0.005, SEVO: −4.6 ± 1.6 %, P = 0.039). There was no significant effect of HAL, ISO or SEVO on I_{to} in ENDO cells.

I_{ss}, measured as the end current in I_{to} recordings, was not significantly different in EPI (1.94 ± 0.09 nA) and ENDO (1.69 ± 0.10 nA) cells. HAL (0.6 mM) significantly increased I_{ss} in EPI (+7.2 ± 2.0 %, P = 0.011) and ENDO (+5.8 ± 0.8 %, P < 0.001) cells. 1 mM SEVO also increased I_{ss} in both EPI and ENDO cells (EPI: +8.6 ± 1.0 %, P < 0.001, ENDO: +8.2 ± 3.1 %, P = 0.024) but 1 mM ISO had no significant effect on I_{ss}.

Reduction of I_{Ca} and an increase in I_{ss} would lead to shortening of APD, whereas inhibition of I_{to} would prolong APD. In ENDO cells where I_{to} is essentially absent, blockade of inward current would predominate, leading to a greater anaesthetic-induced shortening of APD than in EPI cell where both I_{Ca} and I_{to} are inhibited and I_{ss} increased.

Rithalia, A. *et al.* (2001). *Anesthesiology* **95**, 1213–1219.

This work was supported by the British Heart Foundation.

All procedures accord with current UK legislation.

Immunocytochemistry supports the gradient rather than the mosaic model of the assembly of single cells to produce the intact SA node

Halina Dobrzynski, Sally E. Wright, Simon H. Parson, Jue Li, Sandra A. Jones, Matthew K. Lancaster and Mark R. Boyett

School of Biomedical Sciences, University of Leeds, Leeds, UK

It is known that the sinoatrial (SA) node consists of a heterogeneous population of cells in terms of morphology and electrical activity. However, it is not known how the cells are assembled to produce the intact SA node. Two models have been proposed: the mosaic model, which proposes a varying mixture of atrial and SA node cells from the centre to the periphery of the SA node (Verheijck *et al.* 1998), and the gradient model, which proposes no atrial cells within the SA node but the SA node cell type changes from the centre to the periphery of the SA node (Boyett *et al.* 2000). To investigate the make up of the intact SA node, we used immunocytochemistry to map the expression of atrial natriuretic peptide (ANP), neurofilament (NF; a protein found in nerve cells and cardiac pacemaker/conducting tissues), and connexin43 (Cx43; a component of gap junctions responsible for electrical coupling). Rabbits were killed humanely (UK Home Office Schedule 1 method) and the SA node isolated. Ten micrometre serial sections through the SA node were cut at the level of the normal position of the leading pacemaker site and processed for immunocytochemistry. Results were obtained using a Leica confocal microscope. We have previously investigated the expression of Cx45 (another component of gap junctions) as well as Cx43 in tissue sections through the SA node. The results of this study (and our previous results) are summarised in Fig. 1. Figure 1 shows a schematic diagram of a section cut through the atrial muscle of the crista terminalis and the SA node. The atrial muscle (black) expresses ANP but not NF, and the whole SA node (light and dark grey) expresses NF but not ANP. The atrial muscle also expresses Cx43 but not Cx45. The periphery of the SA node (light grey) expresses both Cx43 and Cx45, whereas the centre of the SA node (dark grey) expresses Cx45 but not Cx43.

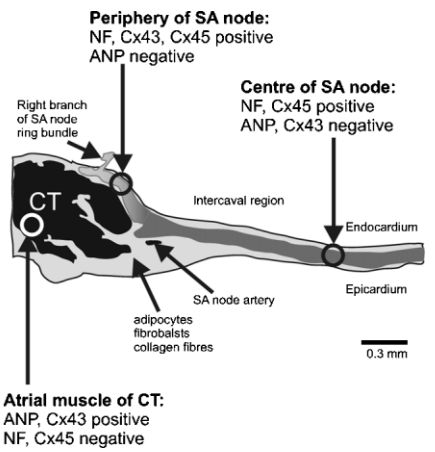

Figure 1. A schematic diagram of a section through the crista terminalis (CT) and intercaval region of rabbit showing distribution of different cell types.

On the basis of these immunocytochemical markers, three cell types can be identified: ANP-positive/NF-negative/Cx43-positive/Cx45-negative (black), ANP-negative/NF-positive/Cx43-positive/Cx45-positive (light grey), and ANP-negative/NF-positive/Cx43-negative/Cx45-positive (dark grey). Our results show that the use of ANP, NF, Cx43 and Cx45 as markers provides no evidence for atrial cells within the SA node – instead in any one area the cells are uniformly of one type. We conclude that immunocytochemistry supports the gradient model to produce the intact SA node.

Boyett, M.R. *et al.* (2000). *Cardiovasc. Res.* **47**, 658–687.

Verheijck, E.E. *et al.* (1998). *Circulation* **97**, 1623–1631.

All procedures accord with current UK legislation.

Absence of ANP protein and mRNA from the rabbit sinoatrial node

James O. Tellez, Rudi Billeter, Sally E. Wright, Payam Shalchi, Mark R. Boyett and Halina Dobrzynski

School of Biomedical Sciences, University of Leeds, Leeds LS2 9JT, UK

Atrial natriuteic peptide (ANP) is produced mainly by the cardiac atria and has been shown to be involved in sodium and volume homeostasis (de Zeeuw *et al.* 1992). The aim of the study was to determine whether ANP is expressed in the sinoatrial (SA) node, the pacemaker of the heart, of the rabbit. Rabbits were killed humanely (UK Home Office Schedule 1 method) and the SA node was isolated. Ten micrometre serial sections through the SA node (approximately at the level of the leading pacemaker site) and surrounding atrial muscle of the crista terminalis were cut. Adjacent SA node sections were examined for ANP protein and mRNA. ANP protein was detected using immunohistochemistry, with a suitable anti-ANP monoclonal IgG (1:100, Biogenesis Ltd, Poole, UK). This showed ANP protein to be present throughout the surrounding atrial muscle, but absent in the SA node (Fig. 1A and B). Similar results were seen in sections from three rabbits. ANP mRNA was localised using *in situ* hybridisation (ISH). Antisense and sense digoxigenin-labelled riboprobes (385 nt) were designed specifically for rabbit ANP mRNA. Signal for ANP mRNA was obtained throughout the atrial muscle using the antisense riboprobe (Fig. 1C). The specificity of the signal was confirmed by the lack of binding of sense riboprobe. With the antisense riboprobe, the ANP mRNA signal was absent from the SA node (Fig. 1D).

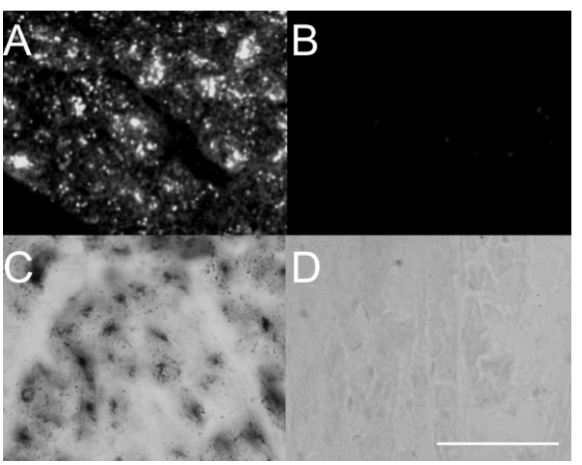

Figure 1. A, ANP protein in crista terminalis. B, absence of ANP protein in SA node. C, ANP mRNA in crista terminalis. D, absence of ANP mRNA in SA node. Fluorescent confocal images (FITC-labelled secondary IgG used), A and B. Brightfield images, (NBT precipitate from alkaline phosphatase reaction), C and D. Scale bar for all panels in D = 25 μm.

Similar results were seen in sections from two rabbits. When the negative regions for ANP protein and mRNA were compared on adjacent sections, they were shown to occupy the same area. High magnification imaging of the ISH staining showed ANP mRNA to be localised in the perinuclear region (presumably in the rough endoplasmic reticulum; Fig. 1C), while immunolabelling showed ANP protein to be present in granules within the cell (Fig. 1A).

It is concluded that (i) ANP is not expressed in the rabbit SA node, (ii) in the SA node expression of ANP is regulated at the level of transcription, and (iii) ANP can be used as a negative marker for rabbit SA node at the level of both mRNA and protein.

de Zeeuw *et al.* (1992). *Kidney Int.* **41**, 1115–1133.

This work was supported by the British Heart Foundation and the Medical Research Council.

All procedures accord with current UK legislation.

Contrasting mechanisms underlie the development of pressure overload *versus* angiotensin II-induced hypertrophy in mice lacking the NADPH oxidase subunit gp91*phox*

J.A. Byrne, D.J. Grieve, J.K. Bendall, A.C. Cave and A.M. Shah

Department of Cardiology, GKT School of Medicine, London, UK

Increased production of reactive oxygen species (ROS) may be involved in the pathophysiology of pressure-overload hypertrophy. We have previously shown that an ROS-generating phagocyte-type NADPH oxidase is expressed in the heart and is involved in the hypertrophic response to subpressor angiotensin II (Ang II) infusion. In this study we compared the response to chronic pressure overload or pressor Ang II infusion in male gp91*phox*$^{-/-}$ mice and matched wild-type C57/Bl6J controls. Adult male mice (16–20 g) underwent (a) suprarenal aortic constriction or (b) 1.1 mg kg^{-1} day^{-1} Ang II or saline infusion via a subcutaneous osmotic minipump. All mice were anaesthetised using 2.5 % isofluorane. The abdominal aorta was constricted with an 8.0 nylon suture tied down onto a 29-gauge needle. Sham animals underwent an identical procedure with the exception of band placement. Perioperative mortality was < 10 % in both groups. Animals were studied a week later (n = 4–6 per group) and were humanely killed according to Home Office guidelines using sodium pentobarbitone (120 mg kg^{-1} I.P.). Data are expressed as means ± S.E.M. and statistical analysis was made using Student's unpaired t test or two-way ANOVA for repeated measures. In all cases $P < 0.05$ was taken to be significant.

Ang II infusion increased systolic blood pressure in both WT (162.1 ± 9.8 *vs.* 132.5 ± 2.2 mmHg; $P < 0.05$) and gp91*phox*$^{-/-}$ mice (138.1 ± 6.0 *vs.* 123.2 ± 3.5 mmHg; $P < 0.05$).

Heart : body weight ratio was significantly increased by Ang II (~24 %) in WT (4.26 ± 0.1 *vs.* 3.44 ± 1.0 mg kg^{-1}; $P < 0.05$) but not in gp91*phox*$^{-/-}$ mice (3.99 ± 0.06 *vs.* 3.72 ± 0.11 mg kg^{-1}; P = n.s.). In line with this, Ang II increased cardiac NADPH oxidase activity in WT (70.7 ± 18.6 %, $P < 0.05$) but not in gp91*phox*$^{-/-}$ mice, −17 ± 13 %). In contrast, aortic banding induced similar increases (~25 %) in LV : body weight ratio in WT (3.91 ± 0.13 *vs.* 3.14 ± 0.11 mg kg^{-1}; $P < 0.05$) and gp91*phox*$^{-/-}$ mice (4.29 ± 0.05 *vs.* 3.38 ± 0.11 mg kg^{-1}; $P < 0.05$). Surprisingly, NADPH oxidase activity was increased after banding in both WT (38 ± 11 %; $P < 0.05$) and gp91*phox*$^{-/-}$ hearts (58 ± 10 %; $P < 0.05$), and was inhibited by diphenyleneiodonium but not reduced by L-NAME in either group. Aortic banding resulted in an increase in gp91*phox* mRNA expression by real time PCR in WT hearts (1.9 ± 0.2 *vs.* 1.3 ± 0.01 arbritary units; $P < 0.05$).WT and gp91*phox*$^{-/-}$ hearts expressed nox 4 mRNA at a similar level, with no significant increases after aortic banding.

These results indicate that whereas a gp91*phox*-containing NADPH oxidase is essential for the development of Ang II-induced cardiac hypertrophy, this enzyme is not required for the development of pressure overload hypertrophy. The increase in ROS production following pressure overload appears to involve an alternative gp91*phox* isoform.

All procedures accord with current UK legislation.

Cardiac contractile dysfunction and fibrosis induced by chronic pressure overload are inhibited in gp91*phox*-null mice

David J. Grieve, Jonathan A. Byrne, Alison C. Cave and Ajay M. Shah

Department of Cardiology, GKT School of Medicine, London, UK

An increase in oxidative stress is implicated in the pathophysiology of left ventricular hypertrophy (LVH). Recent studies suggest that a phagocyte-type NADPH oxidase is an important source of cardiac superoxide production. We investigated the cardiac response to chronic pressure overload in gene-modified mice lacking the gp91*phox* subunit of NADPH oxidase and matched wild-type C57BL/6J controls. Adult male mice (16–20 g) were anaesthetised (2.5 % isofluorane) and the suprarenal abdominal aorta was constricted with an 8.0 nylon suture tied down onto a 29-gauge needle (~70 % constriction). Sham animals underwent an identical procedure with the exception of band placement. Perioperative mortality was < 10 % in both groups. Animals were studied 2 weeks later (n = 6–8 per group) and were killed humanely according to Home Office guidelines, using sodium pentobarbitone (120 mg kg^{-1} I.P.). Data are expressed as means ± S.E.M. and statistical analysis was made using Student's unpaired t test or two-way ANOVA for repeated measures, as appropriate. In all cases, $P < 0.05$ was taken to be significant. Aortic banding induced similar (~40 %) significant increases in LV/body weight ratio in wild-type (4.57 ± 0.29 *vs.* 3.21 ± 0.07 mg g^{-1}) and gp91*phox*$^{-/-}$ mice (4.87 ± 0.18 *vs.* 3.40 ± 0.07 mg g^{-1}). Lung/body weight ratios were unchanged in both groups. Expression of atrial natriuretic factor mRNA (semi-quantitative PCR) was significantly increased to a similar extent in banded wild-type and gp91*phox*$^{-/-}$ mice (1008 ± 138 and 1244 ± 250 %, respectively). However, cardiac interstitial fibrosis (Masson's trichrome staining) was significantly increased only in wild-type bands (144 ± 33 %) but was unchanged in gp91*phox*$^{-/-}$ bands (9 ± 28 %) compared with shams. Cardiac function was studied in isolated ejecting hearts, with measurement of high fidelity LV pressure (1.4 F Millar catheter), aortic and coronary flow. Wild-type bands showed significant systolic and diastolic dysfunction compared with shams (LV dP/dt_{max}: 4395 ± 123 *vs.* 5855 ± 249 mmHg s^{-1}; cardiac work: 7195 ± 648 *vs.* 10 950 ± 712 mmHg ml min^{-1} g^{-1}; LV end-diastolic pressure:

19.4 ± 1.1 *vs.* 15.8 ± 0.9 mmHg; all $P < 0.05$). However, banding did not cause either LV systolic or diastolic dysfunction in gp91*phox*$^{-/-}$ mice (e.g. LV dP/dt_{max}: 5504 ± 445 *vs.* 5584 ± 229 mmHg s^{-1}; LV end-diastolic pressure: 18.2 ± 1.8 *vs.* 19.3 ± 1.3 mmHg; P = n.s.). The development of interstitial fibrosis and LV systolic and diastolic dysfunction in chronic pressure overload are inhibited in gp91*phox*-null mice, despite a similar degree of LVH to wild-type bands. These results suggest that a gp91*phox*-containing NADPH oxidase is involved in the development of both contractile dysfunction and interstitial fibrosis but not hypertrophy *per se* during chronic pressure overload.

All procedures accord with current UK legislation.

Cellular modelling of human atrial tissue remodelling produced by atrial fibrillation

C.J. Garratt, A.V. Holden and H. Zhang

Manchester Heart Centre, Manchester Royal Infirmary, Manchester, School of Biomedical Science, University of Leeds, Leeds LS2 9JT and Biological Physics Group, Department of Physics, PO Box 88, UMIST, Manchester M60 1QD, UK

The functional mechanisms underlying chronic atrial fibrillation (AF) have been described in animal models (Nattel *et al.* 2000) and in humans (Bosch *et al.* 1999). AF is associated with remodelling of ionic channel densities and kinetics, and gap junctional coupling. Remodelling of ionic channels has been proposed to underlie the marked decrease in the action potential duration (APD) and adaptation of the APD restitution curve as well as a decrease in atrial conduction velocity. These are believed to favour the genesis and maintenance of chronic AF by multiple re-entrant wavelets. We used a computational model to test the hypothesis that remodelling of ionic channel properties is quantitatively sufficient to account for the reported changes in APD and APD restitution curves of human atrial cells in chronic AF. The model of Nygren *et al.* (1998) of electrical activity of human atrial cells was modified to incorporate the experimental data of AF-induced changes in ionic channel conductances for $i_{K,1}$ (increased by 250 %), $i_{Ca,L}$ (decreased by 74 %), i_{to} (decreased by 85 %) and kinetics of i_{to} (activation curve shifted by 16 mV), $i_{Ca,L}$ (time constant of fast inactivation increased by 62 %) and i_{Na} (inactivation curve shifted by 10 mV). Action potentials and APD restitution curves for remodelled cells were computed and compared with those obtained for the standard model, and also compared quantitatively with those obtained experimentally. In the model we found that AF induced changes in the ionic channel conductances and kinetics were able to quantitatively reproduce the changes in the APD and APD restitution curve seen in clinical experiments. The AF induced changes in the characteristics of human atrial action potential, such as shortening APD, increase of resting potential (towards more negative) and adaptation of APD restitution curve are quantitatively accounted for by the integrated actions of AF up-regulation of $i_{K,1}$, downregulation of i_{to}, $i_{Ca,L}$ and changed channel kinetics of $i_{Ca,L}$, i_{to} and i_{Na}.

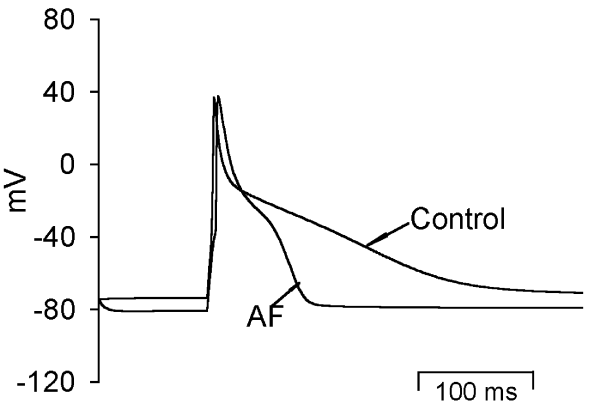

Figure 1. Computed action potential produce by 2 ms, 6 nA current pulse for standard Nygren *et al.* (1998) and AF remodelled human atrial cell.

Bosch, R.F. *et al.* (1999). *Cardiovascular Res.* **44**, 121–131.

Nattel, S. *et al.* (2000). *Annu. Rev. Physiol.* **62**, 51–77.

Nygren, A. *et al.* (1998). *Circ. Res.* **82**, 63–81.

Regional differences in excitation–contraction coupling in the guinea-pig left ventricle

H.L. Wallis, C. Sears and S. Bryant

John Radcliffe Hospital, University of Oxford, Oxford, UK

Although it is well established that there is heterogeneity in the electrophysiological characteristics of single myocytes across the left ventricular free wall (LV), little is known about how these differences may influence excitation–contraction coupling (E–C C) within the heart.

E–C C was investigated in myocytes isolated from basal sub-endocardial (ENDO), mid-myocardial (MID) and sub-epicardial (EPI) regions of the guinea-pig LV. Animals were killed humanely. Membrane current and unloaded cell shortening (UCS) were measured using the whole-cell patch-clamp and video-edge detection techniques at 35 ± 1 °C. $I_{Ca,L}$ and UCS were elicited by 300 ms step depolarisations to test potentials ranging between −50 and +80 mV. Sarcoplasmic reticulum (SR) Ca^{2+} load was assessed by integration of the caffeine-induced current in the presence of carboxyeosin (20 μM). The Na–Ca exchanger current (I_{NCX}) was elicited by a descending ramp protocol (+80 to −120 mV) and assessed as the Ni^{+}-sensitive current. SR Ca-ATPase (SERCA2a), phospholamban (PLB) and NCX protein levels were determined using quantitative Western blot techniques and expressed relative to GAPDH. Data are presented as means ± S.E.M. (n), ANOVA significance level $P < 0.05$.

Peak amplitude of UCS was greater in EPI compared with ENDO myocytes ($P < 0.05$, Fig. 1A). The maximal rate of both contraction and relaxation was faster in EPI than in ENDO myocytes ($P < 0.05$). Although $I_{Ca,L}$ density (Fig. 1B) and myofilament sensitivity were similar between the regions, SR Ca^{2+} load was significantly greater in EPI compared with ENDO myocytes ($P < 0.002$, Fig. 2A). In the presence of carboxyeosin, the integral of the caffeine-induced inward current was significantly increased in EPI but unaltered in ENDO myocytes

($P < 0.05$, Fig. 2A), suggesting that the contribution made by the sarcolemmal Ca-ATPase to Ca^{2+} extrusion was greater in EPI than in ENDO myocytes.

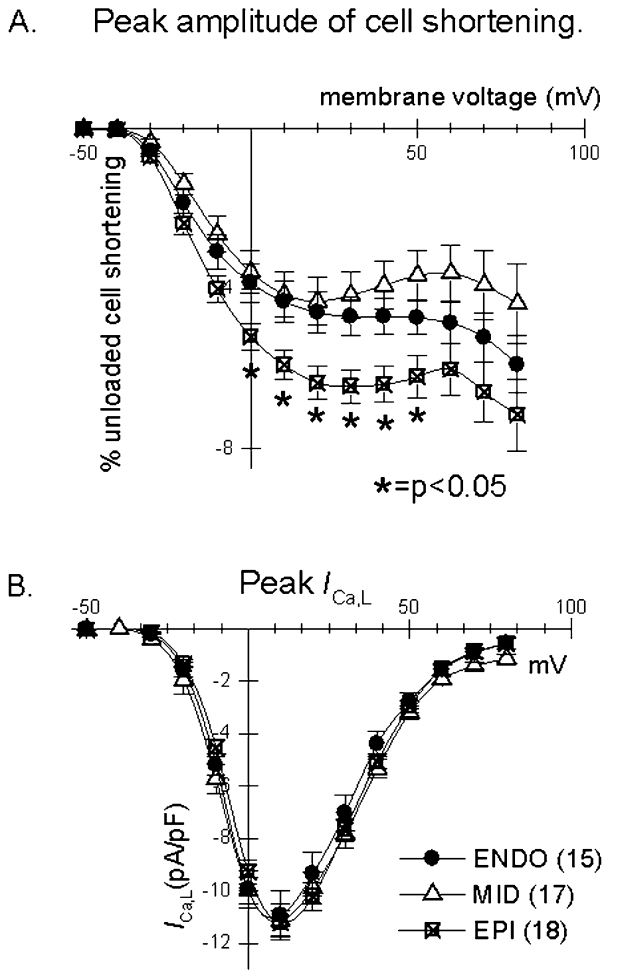

Figure 1. *A,* regional assessment of peak unloaded cell shortening. *B,* regional assessment of L type calcium current density.

I_{NCX} density was greater in ENDO than in EPI myocytes, ($P < 0.001$) in both 'forward' and 'reverse' modes (Fig. 2B), consistent with the greater total NCX protein content in ENDO than EPI myocytes.

SERCA2a protein level was greater in EPI compared with ENDO myocytes, but PLB was greater in ENDO compared with EPI myocytes. The resultant reduction in the PLB : SERCA2a ratio (a useful indicator of contractility and relaxation) in EPI compared with ENDO myocytes is consistent with the faster kinetics in EPI myocytes.

These data show that contraction amplitude is greater and relaxation faster in EPI than ENDO myocytes. This is in part attributable to a greater SR Ca^{2+} load and a reduced PLB:SERCA2a ratio in EPI myocytes. In addition, $I_{Na\text{-}Ca}$ density and NCX protein levels were greater in ENDO myocytes, which may underlie a greater propensity for arrhythmias seen in ENDO myocytes.

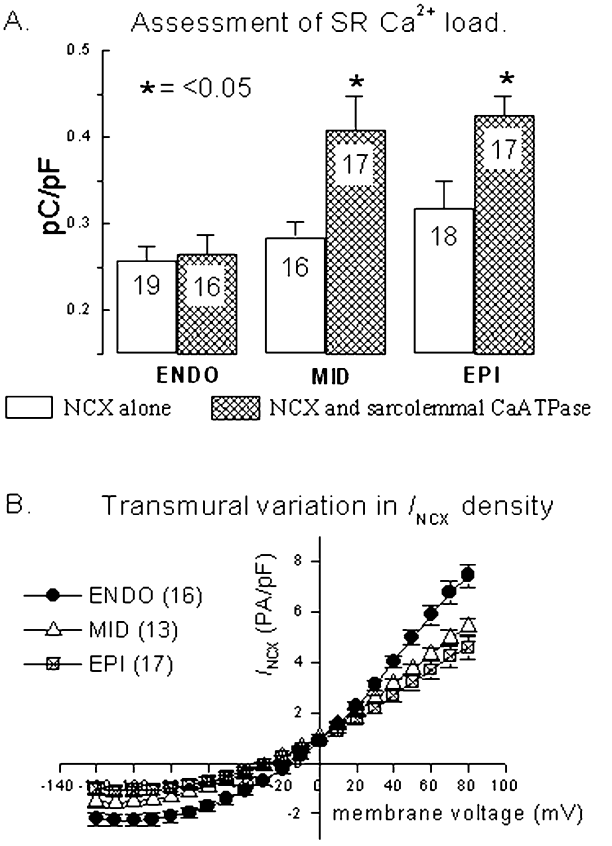

Figure 2. *A,* regional assessment of trans-sarcolemmal calcium extrusion mechanisms. *B,* regional assessment of sodium–calcium exchanger current density.

All procedures accord with current UK legislation.

Non-uniform fibre rotation in swine RV subepicardium and its implications for electrical conduction

Stephen B. Simons*, Fred Vetter†, Sergey Mironov*, Christopher Hyatt* and Arkady M. Pertsov*

**Department of Pharmacology, SUNY Medical Upstate University, Syracuse, NY 13210 and †Department of Electrical and Computer Engineering, University of Rhode Island, Kingston, RI 02881, USA*

It is known that myocardial fibres rotate counterclockwise through the wall of the heart. Abrupt rotations in fibre orientation are implicated in arrhythmogenesis and should be considered during measurements of conduction velocity in ventricular myocardium. We combined histology, optical mapping and computer modelling to test the hypothesis that abrupt changes in subepicardial fibre orientation are responsible for unusual diamond-shaped activation patterns in swine RV.

Young pigs ($n = 7$) were heparinized (500 IU, I.V.) and subsequently anaesthetized with sodium pentobarbital (35 mg kg^{-1} I.V.). All procedures were conducted in agreement with the Guide for the Care and Use of Laboratory Animals (NIH

publication no. 85–23, revised 1996). The heart was quickly removed and the RV free wall excised and cannulated through the right coronary artery. Preparations were then perfused and superfused with an oxygenated Tyrode solution, and stained with the voltage-sensitive dye di-4-ANEPPS. Contractions were inhibited using diacetyl monoxime (15 mmol l^{-1}). Optical signals were recorded from the epicardial surface with a CCD video camera at 800 fr s^{-1}. After completion of the experiments preparations were sectioned using traditional histological methods. Fibre orientation of each section was determined using an automatic algorithm. To simulate voltage-dependent optical signals, measured fibre angles were introduced into a computer model comprised of a three-dimensional model of electrical propagation and a multi-scattering light transport model. Electrical action potential waveforms were generated using Fenton-Karma kinetics. Optical action potential waveforms were obtained by convolving optical point spread functions, derived from the light transport model, with the computed three-dimensional distribution of the transmembrane potential.

In the majority (n = 4/7) of preparations, we observed an abrupt change in fibre angle (70–90 ± 10 deg (S.D.)) at subepicardial depths of ~500 μm (Fig. 1A). These large magnitudes of rotation produced unusual diamond and quasi-rectangular-shaped activation patterns during epicardial point stimulation. The shape of wavefront directly correlated with the amount of rotation observed, with diamond shapes displaying the most rotation. Insertion of histological data into computer models accurately reproduced experimental observations (Fig. 1B).

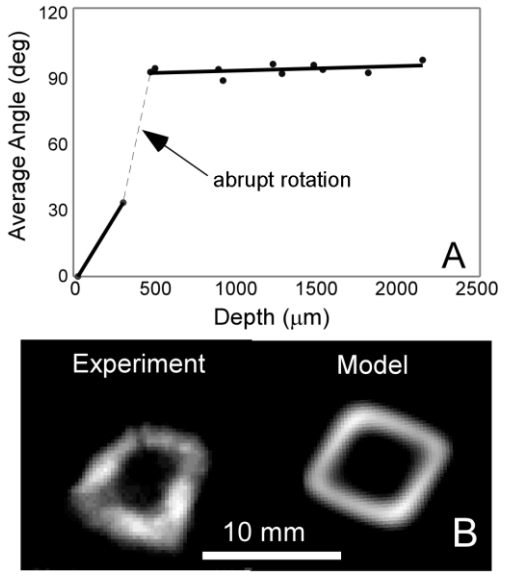

Figure 1. Snapshots of the excitation front produced by epicardial point stimulation. Grey levels represent the relative rates of depolarisation.

Fibre rotation in swine RV is non-uniform, resulting in unusual patterns of electrical activation on the epicardial surface. This is important for understanding electrical propagation in the three-dimensional wall of the heart, and fibre architecture in the RV free wall.

This work was supported by Grant 2PO1-HL-39707 from the National Heart, Lung and Blood Institute of the National Insitutes of Health.

All procedures accord with current National guidelines.

Torso mapping can identify changes in ventricular activation-recovery intervals during regional ischaemia that are not detected using the electrocardiogram in the anaesthetised pig

Martyn P. Nash, Chris P. Bradley and David J. Paterson

University Laboratory of Physiology, Parks Road, Oxford OX1 3PT, UK

Diagnosing myocardial ischaemia with a standard 12-lead ECG may result in false negatives due to its poor spatial resolution. We correlated changes in torso and epicardial electrograms (EGs) during regional ventricular ischaemia in an anaesthetised (α-chloralose, 100 mg kg^{-1} I.V.) 29 kg pig that was artificially ventilated and thoracotomised. The animal was killed humanely at the end of the experiment. A suture snare was used to ligate the left anterior descending (LAD) coronary artery and an elasticized sock containing 127 unipolar electrodes was placed over the epicardium. The chest was reclosed and a vest containing 256 ECG electrodes was fitted to the torso. Simultaneous arrays of torso and epicardial EGs were recorded every 20 s during 4 min of LAD occlusion, followed by a period of reperfusion. Epicardial activation-recovery intervals (ARIs) and torso Q-T intervals (QTIs) were calculated from the EGs. Data were sampled at 2 kHz using a UnEmap data aquisition system and visualized using anatomically accurate computational models of the ventricular epicardium (Nash *et al.* 2001) and the porcine thorax (Nash *et al.* 2002).

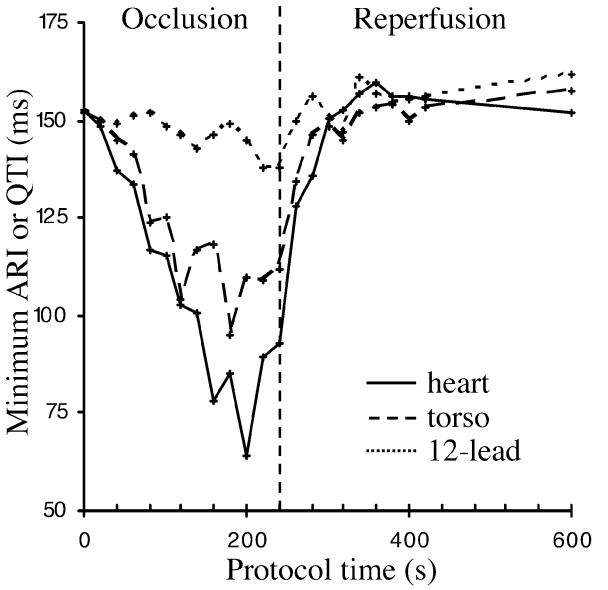

Figure 1. Epicardial ARI and torso QTI changes during LAD occlusion and reperfusion. The minimum ARI (continuous line) steadily decreased during occlusion and this was associated with a marked decrease in the minimum QTI (dashed line), but was not well reflected in the standard 12-lead QTI (dotted line). Maximum and mean values (not shown) remained relatively unchanged during the entire protocol.

LAD occlusion caused the minimum epicardial ARI to steadily decrease (see Fig. 1), whilst the location of this minimum shifted from the posterio-basal ventricular muscle (control) to the middle of the ischaemic region on the anterio-apical myocardium. These changes were associated with a steady decrease in the minimum torso QTI as it moved from the shoulder region (control) to the sternum. The 12-lead QTI was relatively unchanged. All electrical activity was fully restored

following 6 min of reperfusion. We conclude that high spatio-temporal resolution torso mapping can detect cardiac ischaemia that is not always identifiable using indices derived from standard ECG limb leads.

Nash, M.P. *et al.* (2001). *J. Appl. Physiol.* **90**, 287–298.

Nash, M.P. *et al.* (2002). *Chaos, Solitons and Fractals* **13**, 1735–1742.

This work was funded by The Wellcome Trust and the British Heart Foundation. The investigation was performed under a Home Office Project Licence PPL 30/1133.

All procedures accord with current UK legislation.

Effect of detubulation on phospholamban phosphorylation in rat ventricular myocytes

F. Brette*, P. Rodriguez†, J. Colyer† and C.H. Orchard*

**School of Biomedical Sciences and †School of Biochemistry and Molecular Biology, University of Leeds, Leeds LS2 9NQ, UK*

Phospholamban (PLB) regulates the cardiac sarcoplasmic reticulum Ca-ATPase: phosphorylation of PLB at Ser^{16} or Thr^{17}, by protein kinase A and Ca–calmodulin-dependent protein kinase II (CaMKII), respectively, stimulates the pump. Previous work (Drago *et al.* 1998) has shown that PLB phosphorylated at Thr^{17} is localised at the Z-lines, adjacent to the t-tubules. Because Ca influx pathways are concentrated in the t-tubules, it seemed possible that this pattern of phosphorylation was due to local Ca^{2+} entry. We therefore investigated the pattern of phosphorylation in detubulated myocytes.

Ventricular myocytes were isolated from the hearts of Wistar rats, which were killed humanely by a Schedule 1 method, and detubulated as described previously (Kawai *et al.* 1999). Control and detubulated myocytes were stimulated at 0.5 Hz for 5 min in control perfusate or perfusate plus 1 μM isoproterenol (ISO) at room temperature. The cells were then fixed, permeabilised and PLB location determined using primary antibodies against phospholamban (A1), phospholamban phosphorylated at Ser^{16} (PS-16) or Thr^{17} (PT-17) and FITC-labelled secondary antibodies, which were visualised using confocal microscopy. Data are presented as means ± S.E.M. of n cells. Statistical significance was determined using Student's t test or Mann-Whitney test as appropriate.

A1 antibody showed regular transverse striations in control and detubulated cells, at intervals of 1.65 ± 0.02 μm ($n = 10$) and 1.65 ± 0.04 μm ($n = 9$, $P > 0.05$), respectively, with no significant difference in mean fluorescence between control and detubulated cells. PT-17 antibody showed similar transverse striations in control and detubulated cells in the absence and presence of ISO, although the intensity of staining was significantly greater in the presence of ISO; these striations occurred at intervals of 1.68 ± 0.02 μm ($n = 15$) and 1.67 ± 0.02 μm ($n = 17$, $P > 0.05$) in control and detubulated cells, respectively, in the presence of ISO. A similar pattern of staining and response to ISO was observed using the PS-16 antibody in control and detubulated cells, although some staining of the nuclear envelope was also visible. Specificity of antibody staining was confirmed by competition with the appropriate peptide.

These data suggest that PLB is localised close to the Z-lines. This distribution, and the pattern of phosphorylation, is unchanged by detubulation. Thus it appears likely that phosphorylation of Thr^{17} is not due to local Ca signalling at the t-tubule, but to the distribution of PLB and an increase in global [Ca] within the cell.

Drago, G.A. *et al.* (1998). *Ann. N. Y. Acad. Sci.* **853**, 273–279.

Kawai, M. *et al.* (1999). *Am. J. Physiol.* **277**, H603–609.

This work was supported by The Wellcome Trust.

All procedures accord with current UK legislation.

Mechanical and electrophysiological effects of BDM and cytochalasin-D in the rabbit heart

S. Kettlewell, N.L. Walker*, F.L. Burton*, S.M. Cobbe* and G.L. Smith

*IBLS, University of Glasgow, Glasgow G12 8QQ and *Department of Medical Cardiology, Glasgow Royal Infirmary, Glasgow G32 2ER, UK*

Application of optical mapping techniques and fluorescent dyes to image membrane potential and other modalities requires a relatively immobile preparation. Pharmacological interventions that reduce motion artifact may also affect electrophysiology. The effect of 2,3-butanedione monoxime (BDM) (1, 5 and 20 mM) and cytochalasin-D (cyto-D) (1, 3 and 5 μM) on electrophysiology and contractility were assessed in Langendorff-perfused rabbit hearts ($n = 4$).

NZ White rabbits (1.5–2 kg) were killed by I.V. administration of sodium pentobarbitone (100 mg kg^{-1}) with 1000 IU heparin. Monophasic action potentials (MAPs) were recorded from the basal epicardial surface of the left ventricle. MAP duration was measured at 90% repolarisation ($MAPD_{90}$). Conduction delay (CD) was measured as the time between right ventricular basal stimulus artifact and the MAP upstroke. Left ventricular developed pressure (LVDP) was expressed as a percentage of the control value. The effect of 20 mM BDM ($n = 3$) and 3 μM cyto-D ($n = 4$) on restitution was assessed with 16 S1 stimuli at 350 ms intervals followed by an extra stimulus S2. S1–S2 was increased incrementally from 70 to 600 ms. An exponential curve was fitted to a graph of $MAPD_{90}$ against preceding diastolic interval.

Table 1. Effect of BDM and Cyto-D on conduction delay, $MAPD_{90}$ and left ventricular developed pressure.

		CD (ms)	$MAPD_{90}$ (ms)	LVDP (% Control)
BDM (mM)	C	33.1±1.2	119.6±1.7	100
	1	35.4±2.4	103.7±9.5	67.0±21.1
	5	42.2±1.7*	116.0±6.5	63.1±3.2
	20	43.6±1.4**	112.7±5.0	23.0±18.4**
Cyto-D (μM)	C	31.2±2.0	121.3±2.8	100
	1	35.8±1.8	110.2±2.8	77.4±11.8*
	3	37.2±1.5*	128.3±2.8*	26.0±5.3***
	5	39.3±2.6**	139.3±1.8**	12.8±3.5***

Basic Cycle Length 350ms. Repeated measures ANOVA. *P<0.05, **P<0.01, ***P<0.001.

BDM increased CD in a dose-dependent manner; cyto-D had a smaller but significant effect. $MAPD_{90}$ was unaffected by BDM, but at 5 μM cyto-D caused a significant prolongation (Table 1). Both agents increased the time constant. Maximum $MAPD_{90}$ was decreased in 20 mM BDM and increased in 3 μM cyto-D (Table 2).

Table 2. Effect of BDM and Cyto-D on restitution parameters.

	Control	20mM BDM	3μM Cyto-D
Min $MAPD_{90}$ (ms)	109.7±2.5	100.0±2.5*	103.0±2.7
Max $MAPD_{90}$ (ms)	125.1±4.2	111.9±5.3*	124.8±5.7
Time constant (ms)	7.4±1.6	23.2±3.7*	40.4±5.2**
ERP (ms)	112.9±5.8	81.7±3.3*	135.0±6.6

Paired Student's t-test. *P<0.05, **P<0.01.

Both BDM and cyto-D have substantial negative inotropic effects. Any flattening of the restitution curve by such agents may have anti-arrhythmic consequences.

All procedures accord with current UK legislation.

Biphasic actions of cADP-ribose phosphate on contraction in guinea-pig isolated ventricular myocytes

A. Macgregor, S. Rakovic, G.C. Churchill, A. Galione and D.A. Terrar

Department of Pharmacology, University of Oxford, Mansfield Road, Oxford OX1 3QT, UK

cADP-ribose (cADPR) has been shown to regulate calcium release from intracellular stores in a variety of mammalian cells. However, little is known regarding possible actions of the phosphate analogue, cADPR-P. The aim of this study was to investigate any possible effects of cADPR-P on guinea-pig ventricular myocytes.

Male guinea-pigs were killed by cervical dislocation following stunning, and myocytes isolated enzymatically from the ventricles of the hearts. Cells were superfused with physiological solution containing 2.5 mM calcium (36 °C) and patch clamped (using either conventional whole-cell or amphotericin-permeabilized configurations). Action potentials were stimulated at 1 Hz. Cell shortening was measured from a video image of the cell using an edge-detection system. Sarcoplasmic reticulum (SR) loading was assessed under voltage-clamp conditions, by measuring the integral of the inward current generated in response to rapid application of 20 mM caffeine. Data are quoted as means ± S.E.M. and statistical significance assessed using Student's paired *t* test.

cADPR-P caused a concentration-dependent (100 nM to 100 μM in the pipette) increase in cell contraction when applied using conventional whole-cell patch (control measurements made within 30 s of membrane rupture when little cADPR-P is expected to have entered the cytoplasm). 10 μM cADPR-P increased contraction by 32 ± 8 % after 3 min ($n = 6$, $P < 0.05$). In a second series of experiments, control measurements were made in the permeabilized patch after which the membrane was ruptured to allow cADPR-P entry to the cytoplasm. At low concentrations (10 nM to 1 μM), there was a significant decrease in cell contraction. 100 nM cADPR-P decreased cell contraction by 36 ± 7 % after 3 min ($n = 6$, $P < 0.05$). At higher concentrations (10 and 100 μM) there was a significant increase in cell contraction. 10 μM cADPR-P increased cell contraction by 26 ± 5 % after 3 min ($n = 10$, $P < 0.05$). In six of these cells in which 10 μM cADPR-P increased contraction by 28 ± 5 % ($P < 0.05$), there was no significant change in SR loading (6 ± 7 %, $n = 6$, $P > 0.05$). In contrast, there were no significant changes in cell contraction over this time period if cADPR-P was excluded from the patch pipette in either series of experiments.

These data are consistent with a biphasic action of cADPR-P on contraction of guinea-pig ventricular myocytes, with low concentrations reducing contraction magnitude, and higher concentrations enhancing it. The enhancement of contraction was not associated with an increase in loading of the SR with calcium. Whether cADPR-P exerts its effects through the same mechanism as cADPR or independently remains to be determined.

This work was supported by the British Heart Foundation and The Wellcome Trust.

All procedures accord with current UK legislation.

Ca^{2+} content of the sarcoplasmic reticulum (SR) in isolated left ventricular myocytes during catecholamine-induced cardiac hypertrophy

A. Chorvatova, G. Hart and M. Hussain

Department of Medicine, University of Liverpool, Liverpool L69 3GA, UK

We have previously shown that Na^+–Ca^{2+} exchange current ($I_{Na/Ca}$) density is increased (Chorvatova *et al.* 2001) and that L-type Ca^{2+} current (I_{Ca}) remains unchanged during catecholamine-induced hypertrophy (Meszaros *et al.* 1997). The present study investigated the effects of hypertrophy on Ca^{2+} release and Ca^{2+} content of the SR to determine the consequences of increased $I_{Na/Ca}$.

Hypertrophy was produced by daily injections of isoprenaline (5.0 mg kg^{-1}; I.P.) for 7 days. Rats were stunned and killed by cervical dislocation (Schedule 1; Scientific Procedures Act, 1986). The hearts were isolated and digested by protease and collagenase treatment to isolate myocytes. Cells were loaded with fura-2 AM (5 mmol l^{-1}; 15 min) and field stimulated (0.5 Hz, 2 ms pulse width). Fluorescence ratio (F_{340}/F_{380}) was converted to $[Ca^{2+}]_i$ by *in vivo* calibration. Ca^{2+} content of the SR was assessed by rapid application of 10 mmol l^{-1} caffeine. Composition of the extracellular solution was (mmol l^{-1}): NaCl, 140; KCl, 5.4; $MgCl_2$, 1.0; $CaCl_2$, 1.0; glucose, 10.0 and Hepes, 10.0; pH 7.35 with NaOH. Experiments were conducted at 35 °C. Data are shown as means ± S.E.M. and analysed by Student's *t* test for unpaired data.

Membrane capacitance, determined by patch clamp, was increased by 18 % in hypertrophied myocytes (151.5 ± 6.8 pF, $n = 32$ in control *vs.* 178.8 ± 8.8 pF, $n = 49$ hypertrophy, $P < 0.05$). Peak amplitude of the Ca^{2+} transients was 457 ± 23 nmol l^{-1} ($n = 24$) in control and 685 ± 52 nmol l^{-1} ($n = 18$) in hypertrophied myocytes, representing an increase of ~50 % ($P < 0.05$). Resting $[Ca^{2+}]_i$ was unchanged in the two groups of cells (231 ± 20 in control *vs.* 218 ± 15 nmol l^{-1} hypertrophy). The time constant (t) for the decline of the Ca^{2+} transients was also not significantly different between the two groups (204 ± 9 ms in control and 187 ± 10 ms in hypertrophy). In experiments where caffeine was used to estimate SR Ca^{2+} content, integrals of the Ca^{2+} transients elicited by 10 mmol l^{-1} caffeine were increased in hypertrophied myocytes (control, 738.7 ± 27.9 nmol l^{-1} ms, $n = 24$ *vs.* hypertrophy, 947.8 ± 65.3 nmol l^{-1} ms, $n = 16$, $P < 0.05$). However, increased SR Ca^{2+} content, also determined by measuring caffeine-induced sarcolemmal current, was not observed when myocytes were held and stimulated from −40 mV.

Data show that SR Ca^{2+} release and Ca^{2+} content were increased in myocytes from hypertrophied hearts, despite an increase in $I_{Na/Ca}$ density and unchanged I_{Ca}. The observed increase in SR Ca^{2+} content may therefore result from increased Ca^{2+} entry via reverse Na^+–Ca^{2+} exchange, and enhance Ca^{2+}-induced Ca^{2+} release from the SR.

Chorvatova, A. *et al.* (2001). *J. Physiol.* **533.P**, 28*P*.
Meszaros, J. *et al.* (1997). *Exp. Physiol.* **82**, 71–83.

All procedures accord with current UK legislation.

Time course of L-type calcium current inactivation during the action potential is preserved in left ventricular hypertrophy

R. Snowdon, M. Hussain and G. Hart

Department of Medicine, University of Liverpool, Daulby Street, Liverpool L16 3GA, UK

The time course of the L-type calcium current (I_{Ca}) inactivation has been reported as prolonged in cardiac hypertrophy (Hart, 1994). These experiments, however, used rectangular voltage steps, and usually intracellular Ca^{2+} buffering. In this study we used the action potential clamp technique to investigate the inactivation of I_{CaL} in left ventricular myocytes enzymatically isolated from a model of mild left ventricular hypertrophy in the guinea-pig.

Hypertrophy was induced by constriction of the abdominal aorta below the renal arteries with a silver clip (i.d. 0.5 mm) for 20 weeks; sham animals (control) underwent the same procedure without clip placement (Bryant *et al.* 1997). Surgery was performed under general anaesthesia (Hypnorm, 1 ml kg^{-1} and ketamine, 5 mg kg^{-1}, I.M.). The guinea-pigs were humanely killed by pentobarbitone overdose (I.P., 280 mg kg^{-1}). Current and voltage clamp experiments where conducted at 35 °C, using K^+-based pipette solutions free of Ca^{2+} buffering, during whole-cell patch-clamp.

Action potentials, recorded from hypertrophied and control myocytes, were time-averaged and applied as the command potential during a double-pulse protocol where the action potential waveform was interrupted, at various time intervals, by a depolarization step to +10 mV (Linz *et al.* 1998). Cd^{2+}-sensitive I_{Ca}, obtained during the step pulse, was plotted as a function of the maximal available I_{Ca} to obtain the inactivation variable (f). Myocytes from clipped and sham animals were clamped with their own respective action potentials, both with a functional SR and also following inhibition of the SR with ryanodine and thapsigargin (1 μmol l^{-1}).

There was no difference in the degree of I_{Ca} inactivation under physiological conditions between hypertrophy ($n = 8$) and control ($n = 9$) at any time point until control myocytes enter phase 3 of the action potential. With the SR inhibited I_{Ca} inactivation follows a slower time course in hypertrophy after the first 25 ms, becoming significant by 90 ms (hypertrophy 0.39 ± 0.03, control 0.30 ± 0.02, mean ± S.E.M., $n = 8$; $P < 0.05$, Student's unpaired t test). The SR-dependent component, obtained by subtraction, was initially similar at 5 ms but thereafter was greater in hypertrophy (51 ms, hypertrophy 0.79 ± 0.03, control 0.88 ± 0.03; $P < 0.05$).

The time course of I_{Ca} inactivation during the action potential is unchanged in this model of hypertrophy, despite very different relative contributions to the Ca^{2+}-dependent inactivation of I_{Ca}, the SR component being increased and the channel component being reduced in hypertrophy.

Bryant, S.M. *et al.* (1997). *Cardiovasc. Res.* **35**, 315–323.
Hart, G. (1994). *Cardiovasc. Res.* **28**, 933–946.
Linz, K.W. *et al.* (1998). *J. Physiol.* **513**, 425–442.

All procedures accord with current UK legislation.

A putative modulatory effect of external potassium ions on the cardiac Na^+–Ca^{2+} exchanger

Yin Hua Zhang and Jules C. Hancox

Department of Physiology and Cardiovascular Research Laboratories, School of Medical Sciences, University Walk, Bristol BS8 1TD, UK

Differences in intracellular calcium release and removal within the sinoatrial node

M.K. Lancaster, S.A. Jones and M.R. Boyett

School of Biomedical Sciences, University of Leeds, Leeds LS2 9JT, UK

Previously we reported correlations between cell size and properties of the spontaneous intracellular calcium transient for single cells isolated from the rabbit sinoatrial node (SAN) (Lancaster *et al.* 2001). The aim of the present study was to investigate the mechanisms responsible for these. Single SAN cells were isolated from New Zealand White rabbits humanely killed by intravenous overdose of anaesthetic. At 37 °C cells contracted spontaneously and intracellular calcium transients were observed using the fluorescent indicator fluo-3. Cell size was determined from the projected video image of the cell, in μm^2. Sarcoplasmic reticulum (SR) calcium content was released by rapid application of 20 mM caffeine. For analysis data were divided about the mean cell area (611 ± 28 μm^2 (mean ± S.E.M.)) and classed as small or large cells for comparison using Student's t test (unpaired). Significant correlations, as assessed using a linear regression, were found between the amplitude of the spontaneous calcium transient and cell size ($P < 0.0001$; $n = 39$) and the amplitude of the caffeine-evoked transient and cell size ($P < 0.0001$; $n = 39$). Large cells had a larger spontaneous and caffeine transient amplitude ($P < 0.01$) than small cells. The spontaneous calcium transient expressed as a fraction of the caffeine transient significantly correlated with cell size ($P = 0.03$; $n = 39$) large cells having a smaller fractional release of the total SR content with each spontaneous transient ($P < 0.001$). The time constant for the decay of the caffeine transient correlated with cell size both in the presence and absence of nickel ($P = 0.04$ in both cases, $n = 39$ and $n = 19$, respectively), the transient decaying more slowly in small cells ($P = 0.02$). In some instances it was not possible to obtain reliable data for the decay of the caffeine response due to the rapid resumption of spontaneous activity in the maintained presence of caffeine. From the rate constants for the decay of the caffeine transient in the absence and presence of 10 mM nickel, used to block the sodium calcium exchanger, the relative contributions of the sarcolemmal calcium ATPase and sodium calcium exchanger to cytoplasmic calcium removal were calculated. Calcium ATPase removed a mean of 19 ± 0.6 %, sodium calcium exchanger 81 ± 0.6 %. Significant correlations were found between both the calcium ATPase ($P < 0.001$) and sodium calcium exchange activity ($P = 0.006$)

and cell size. Smaller cells had a smaller calcium removal by the calcium ATPase ($P = 0.02$). Previous work (Bleeker *et al.* 1980) reported a correlation between cell size and location, smaller cells being located towards the centre of the SAN larger cells in the periphery. The results are therefore indicative of a low SR calcium content in cells from the centre of the SAN, lower sarcolemmal calcium transporter activity and a change in the relative contribution of the cellular sarcolemmal calcium transport systems from the periphery to the centre. The recruitment of the SR calcium content with each spontaneous depolarisation is greater in the central cells. These results add further intrigue to the problem of understanding the regulation of intracellular calcium within the mammalian SAN and the role it plays.

Bleeker, W.K. *et al.* (1980). *Circ. Res.* **46**, 11–22.
Lancaster, M.K. *et al.* (2001). *J. Physiol.* **533.P**, 30*P*.

This work was supported by the British Heart Foundation.

All procedures accord with current UK legislation.

Comparison of guinea-pig ventricular myocytes and dog Purkinje fibres for *in vitro* assessment of the potential of compounds to prolong QT interval

D.A. Terrar*, C.M. Wilson, S.G. Wilson and B.M. Heath

*Department of Safety Pharmacology, GlaxoSmithKline, The Frythe, Welwyn, Herts AL6 9AR and *University Department of Pharmacology, Mansfield Road, Oxford OX1 3QT, UK*

The *in vitro* measurement of action potential duration is one test system used for assessing the potential of compounds to cause QT prolongation and torsade de pointes arrhythmias in man. The aim of this study was to compare the effect of compounds known to prolong QT and cause torsade arrhythmias through inhibition of I_{Kr}/HERG channels on action potential parameters recorded from guinea-pig ventricular myocytes (VM) and dog Purkinje fibres (PF) under the same conditions.

Cardiac PF were removed from the ventricles of dogs killed with an overdose of sodium pentobarbitone. Ventricular myocytes were isolated from hearts removed from guinea-pigs following stunning and cervical dislocation. The dog PF and guinea-pig VM were superfused with physiological salt solution at 36–37 °C containing (mM): NaCl 125; KCl 5.4; $CaCl_2$ 1.8; $MgCl_2$ 1.0; NaH_2PO_4 1.2; $NaHCO_3$ 25; D-glucose 5.5 (pH 7.4; gassed with 95 % O_2 and 5 % CO_2). Action potentials were stimulated at a frequency of 1 Hz and recorded with microelectrodes containing 3 M KCl (PF) or 1 M $KMeSO_4$ with 10 mM KCl (VM). Data are means ± S.E.M.

The effect of dofetilide, sparfloxacin, sotalol and cisapride on action potential duration at 90 % repolarisation (APD_{90}) in dog PF and guinea-pig VM is shown in Figs 1 and 2. Dofetilide and sotalol caused a greater prolongation of APD_{90} in dog PF compared with guinea-pig VM: dofetilide (100 nM) increased APD_{90} by 56 ± 5 % in dog PF and by 23 ± 1 % in guinea-pig VM and sotalol (100 μM) increased APD_{90} by 43 ± 9 % in dog PF and by 29 ± 9 % in guinea-pig VM. Sparfloxacin (1–100 μM) prolonged APD_{90} to a similar extent in both preparations: at 100 μM, APD_{90} was increased by 31 ± 8 % in dog PF and by 26 ± 4 % in guinea-pig VM. The effect of cisapride on APD_{90} was biphasic in both preparations with a small prolongation at lower concentrations which was reversed (VM) or converted to a shortening (PF) at higher concentrations. The maximum cisapride-induced prolongation of APD_{90} occurred at a lower concentration in the guinea-pig VM compared with dog PF. Cisapride and sparfloxacin also reduced the maximum rate of depolarization, indicating an effect on Na channels. This action may have contributed to the biphasic change in APD_{90} observed with cisapride.

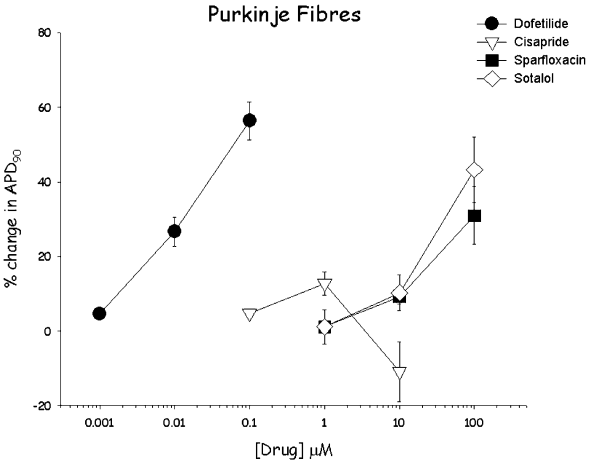

Figure 1.

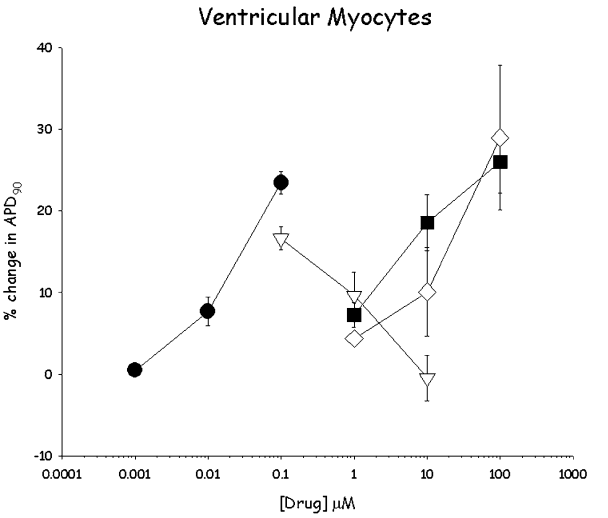

Figure 2.

In conclusion, a prolongation of action potential duration was detected with all four compounds in both preparations. This indicates that the guinea-pig VM is likely to be a suitable preparation in which to assess the possible effect of compounds to prolong action potential duration through inhibition of I_{Kr}/HERG and this preparation may be considered more ethically acceptable for this use than dog cardiac tissue.

All procedures accord with current UK legislation.

Microtubule disruption with colchicine does not modify the cell volume or contractile response to hyposmotic challenge in the adult rat ventricular myocyte

S.D. Bird, S.C. Calaghan and E. White

School of Biomedical Sciences, University of Leeds, Leeds LS2 9JT, UK

In the heart, cell swelling can occur during an acute period of ischaemia-reperfusion. Swelling has been shown to disrupt the microtubule (MT) cytoskeleton in embryonic cardiac myocytes (Larsen *et al.* 2000; Hall *et al.* 2001). Furthermore, MTs have been implicated in the regulatory volume decrease observed following swelling in embryonic myocytes (Hall *et al.* 2001). The aim of the present study was to investigate whether disruption of the MT cytoskeleton during hyposmotic challenge modulated cell swelling and contraction in the adult ventricular myocyte.

Hearts were removed from male Wistar rats following humane killing and ventricular myocytes were isolated by enzymatic disaggregation. Cells were incubated in either 10 μM colchicine (a MT disruptor) or the carrier solution methanol (0.1 %) for 2 h prior to functional studies. Control and colchicine-treated myocytes were stimulated at 0.5 Hz and superfused sequentially with normal physiological Hepes-based solution (290 mosmol), isosmotic solution containing sucrose and low Na^+ (300 mosmol), hypo-osmotic solution (no sucrose, low Na^+; 165 mosmol), and isosmotic solution (23 °C) (± colchicine). Changes in cell size were recorded from a video image of the cell, and cell shortening was measured by video-edge detection.

The mean maximal increase in cell volume of colchicine-treated cells and the time course of this effect, were not significantly different from control cells, during the 18 min exposure to the hyposmotic solution (Fig. 1). The contractile response of cells at maximal cell expansion, observed following 14 min exposure to hyposmotic solution, was not significantly altered for cells exposed to colchicine ($P < 0.05$, Student's unpaired t test).

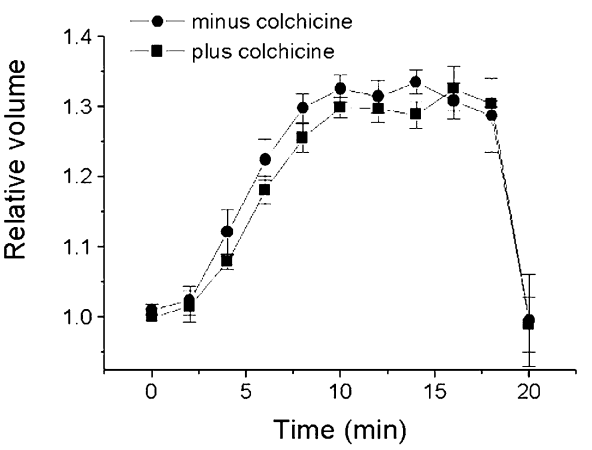

Figure 1. Increase in cell volume (mean ± S.E.M.) relative to the resting volume. Hyposmotic solution applied between zero and 18 min in control ($n = 13$) and colchicine-treated ($n = 15$) cells.

Microtubular disruption with colchicine did not significantly alter cell expansion in adult cardiac myocytes, in constrast with observations in embryonic myocytes (Hall *et al.* 2001). Data from this study suggest that colchicine-sensitive MTs do not modulate the volume or contractile response during hyposmotic swelling in the adult rat cardiac cell.

Hall, S.K. *et al.* (2001). *J. Physiol.* **536.P**, 80*P*.

Larsen, T.H. *et al.* (2000). *Histochem. Cell Biol.* **113**, 479–488.

This study was funded by the British Heart Foundation (S.D.B. and S.C.C.).

All procedures accord with current UK legislation.

Changes associated with ageing in connexin43 protein expression within the sinoatrial node

S.A. Jones, M.K. Lancaster and M.R. Boyett

School of Biomedical Sciences, University of Leeds, Leeds LS2 9NQ, UK

In mammals, a decline in function of the pacemaker of the heart, the sinoatrial node (SAN), is associated with ageing and clinically exhibited as an increase in SAN conduction time and distance from the centre of the SAN to the crista terminalis, resulting in an increase in the velocity of conduction (Alings & Bouman, 1993). These clinical observations could be the result of a decrease in the density of gap junctions. In this study, we have shown expression of the principal cardiac gap junction protein, connexin43 (Cx43), changes with age within the SAN. Data were principally obtained by Western blot and compared with those from conduction maps and immunocytochemistry.

Guinea-pigs aged 1 day to 38 months were humanely killed by anaesthetic overdose. The SAN was removed from the intercaval region between the superior and inferior venae cavae of the right atrium of the heart. The preparation was maintained in oxygenated Tyrode solution at 37 °C and the extracellular electrode was moved at 0.5 or 1 mm intervals and the extracellular potential measured at each point to construct a map of conduction. From the centre of the SAN to the crista terminalis, the distance (1.2 ± 0.2 mm in the 1 day compared with 2.8 ± 0.4 mm in the 38 month animals; $P = 0.005$; $n = 5$) and conduction time (8.6 ± 0.6 ms in the 1 day compared with 17.5 ± 3.7 ms in the 38 month animals; $P = 0.046$; $n = 5$) increased with age. Sections of 14 μm were cut from SAN preparations and labelled using the antibodies anti-Cx43 (Chemicon International, USA) plus anti-IgG conjugated to FITC (Dako, Denmark). Immunofluorescence with confocal laser scanning microscopy demonstrated that anti-Cx43 labelling was absent from the centre of the SAN, increasing from 3.5 ± 0.6 mm^2 in the 1 month to 47.6 ± 2.0 mm^2 in the 38 month animals ($P < 0.02$; $n = 5$), demonstrating a 13-fold increase in area. However, there was no Cx43-negative area in the 1 day animals ($n = 5$). For Western blot, punch biopsy samples (4 mm diameter) were taken from the right atrial appendage and SAN centre from each animal. The paired samples were grouped by age, frozen and ground in liquid nitrogen, prepared in protease inhibitors, separated by 10 % SDS-PAGE, transferred to nitrocellulose and processed with anti-Cx43 plus anti-IgG conjugated to HRP (Dako, Denmark). Bands of Cx43 protein at 43 kDa were detected by chemiluminescence. For each sample the band density was standardised, and each data pair were expressed with the SAN as a proportion of the atrial, for each animal in all age groups. Anti-Cx43 labelled protein for 1 day (60.2 ± 2.2 %) and 1 month (56.3 ± 3.7 %) animals were not significantly different. However, anti-Cx43 labelling of 18 month animals was reduced to 15.1 ± 2.3 %, the 26 month animals to 9.2 ± 1.6 % and the 38 month animals to 5.2 ± 0.7 %, demonstrating an overall reduction of 45 % or 9-fold change

(1 month to 38 months, $P < 0.02$; $n = 5$). Therefore, we have shown a correlation between ageing and the area absent of Cx43 protein expression in the centre of the SAN. This can explain the increase of the SAN conduction time with age. All mean data ± S.E.M. were analysed by Student's unpaired *t* test.

Alings, A.M. & Bouman, L.N. (1993). *Eur. Heart J.* **14**, 1278–1288.

This work was supported by the Medical Research Council and British Heart Foundation.

All procedures accord with current UK legislation.

Improved preservation of rat heart using a phosphate-buffered sucrose-based flush fluid

M. Attia†, Claire Corps*, J.P.A. Lodge† and D.J. Potts*

**School of Biomedical Sciences, University of Leeds and †St James' University Hospital, Leeds, UK*

Previous observations from this laboratory have shown that phosphate-buffered sucrose preservation solutions are effective in protection of liver and kidney from ischaemic damage (Ahmad *et al.* 1997; Song *et al.* 2001).

The safe ischaemic storage time for transplant hearts remains limited. In this study we modified phosphate-buffered sucrose (to make PBSH containing Na_2HPO_4 42.3, NaH_2PO_4 10.67, KH_2PO_4 16, sucrose 100, $MgCl_2$ 5, $CaCl_2$ 0.6, NaCl 12, Diltiazem 0.5 mmol l^{-1}) to provide improved preservation of rat heart and compared its effectiveness with currently used solutions: University of Wisconsin (UW), Lactobionate-mannitol (CS), and St Thomas' no. 2 (STh2). Rats were anaesthetised I.P. with pentobarbitone (60 mg kg^{-1}) and the hearts removed. Hearts were set up in a Langendorff configuration for 5 min perfusion, followed by 15 min working perfusion when control functional observations were made. They were then flushed with preservation fluid, cooled and stored at 4 °C for 6 h. Hearts were then rewarmed for 15 min in a Lagendorff configuration followed by 30 min working during which experimental observations were made. The results are shown in Table 1.

Table 1. % Recovery of aortic flow (AO), coronary flow (CF) and cardiac output (CO)

Solution	AF	CF	CO
PBSH ($n = 6$)	57.1 ± 3.7*	87.7 ± 5.8	66.5 ± 3.3*
UW ($n = 7$)	47.6 ± 5.0	65.3 ± 4.5	51.2 ± 4.4
STh2 ($n = 8$)	37.5 ± 2.5	71.5 ± 5.9	47.3 ± 2.1
CS ($n = 8$)	41.5 ± 3.2	67.8 ± 4.2	47.6 ± 2.0

Values are means ± S.E.M. *$P < 0.05$, ANOVA.

We conclude that PBSH provides better protection from ischaemic damage than Sth2, CS and UW in this model of cardiac ischaemia.

Ahmad, N. *et al.* (1997). *J. Physiol.* **505.P**, 114*P*.

Song, S. *et al.* (2001). *Transplantation Proc.* **33**, 884–885.

This work was supported by the Combined Transplant Fund of St James' Hospital.

All procedures accord with current UK legislation.

Dynamics and pharmacological modulation of spiral re-entry in a two-dimensional sheet of rabbit ventricular muscle perfused *in vitro*

M. Yamamoto, H. Honjo*, I. Sakuma† and I. Kodama*

*School of Biomedical Sciences, University of Leeds, UK, *Research Institute of Environmental Medicine, Nagoya University, Japan and †Graduate School of Frontier Sciences, The University of Tokyo, Japan*

Spiral re-entry plays an important role in the initiation and maintenance of ventricular tachyarrhythmias (Pertsov *et al.* 1993; Fast & Kleber, 1997). However, the precise dynamics of spiral wave propagation in the heart, which determines the behaviour of the activity, are not fully understood. In the present study, we investigated dynamics and pharmacological modulation of spiral re-entry during ventricular tachycardia in a two-dimensional anisotropic subepicardial sheet of ventricular myocardium by optical mapping. Rabbits were killed humanely with an overdose of sodium pentobarbital ($n = 7$). A Langendorff-perfused epicardial layer (~1 mm thick) of rabbit ventricle was made by cryoablation of the endocardial side of the left ventricle. The heart was stained with a potentiometric dye, di-4-ANEPPS, and fluorescence images of the left ventricle were obtained via a high-speed video camera with temporal and spatial resolution of 1.3 ms and 0.1 mm, respectively. In 4 of 7 cases, ventricular tachycardia (VT) induced by cross-field stimulation showed a single circular re-entry around a Z-shaped functional block line (Fig. 1).

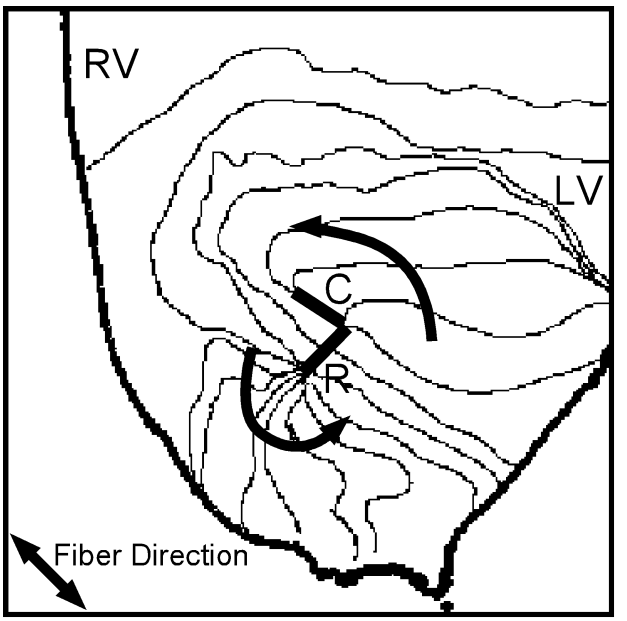

Figure 1. Spiral re-entry around a Z-shaped functional block line during VT. The central portion of the block line was the result of wavefront-tail interactions (refractory block line, R), whereas the peripheral portions were caused by local conduction delay (C). The lower peripheral portion was short and not shown here. Isochrones, 10.7 ms intervals.

The Z-shaped block line was composed of two portions in which the underlying mechanisms were different: the central portion of the block line was created by meandering of the spiral tip along its own refractory tail, and the two peripheral limbs were caused by pronounced local conduction delay at the pivot points. The peripheral block lines were always oriented parallel to the epicardial fibre direction. Double-humped action potentials were recorded at the central block line. Na^+ channel blockade by disopyramide or pilsicainide enhanced local conduction delay at

the pivot points leading to an extension of the peripheral block lines. Around the pivot points, action potentials were widened with steps in the depolarization phase, whereas after making a turn around the pivot points, action potentials were relatively short, giving rise to an excitable gap. These results suggest that the dynamics of spiral re-entry in the two-dimensional ventricular myocardium are mainly determined by (1) tissue anisotoropy, (2) wavefront curvature and (3) the wavefront-tail interaction.

Fast, V.G. & Kleber, A.G. (1997). *Cardiovasc. Res.* **33**, 258–271.
Pertsov, A.M. *et al.* (1993). *Circ. Res.* **72**, 631–650.

All procedures accord with current National guidelines.

Role of protein kinase A-dependent troponin-I phosphorylation in the positive inotropic, lusitropic and diastolic response of isolated mouse hearts to isoprenaline

Joanne Layland, Alison C. Cave, Anna-Marie Perkins, R. John Solaro* and Ajay M. Shah

*King's College London, UK and *University of Illinois at Chicago, USA*

Phosphorylation of cardiac troponin-I (Tn-I) by protein kinase A (PKA) reduces myofilament Ca^{2+} responsiveness and contributes to the myocardial effects of β-adrenoceptor stimulation, in particular acceleration of relaxation. However, the contribution of Tn-I phosphorylation to β-mediated changes in systolic and diastolic function of the whole heart remain unclear. We investigated the effects of isoprenaline (Iso, 10 nM) on contractile function of Langendorff-perfused hearts isolated from male transgenic mice (TG) over-expressing the slow skeletal isoform of Tn-I (lacking PKA phosphorylation sites) and non-transgenic (NTG), male littermate controls ($n \geqslant 6$ per group). Mice were killed by an overdose of sodium pentobarbitone (Sagatal, 120 mg kg^{-1} I.P.). Hearts were perfused at constant coronary perfusion pressure (75 mmHg) and isovolumic left ventricular pressure (LVP) was measured at varying LV volumes using an intraventricular balloon connected to a pressure transducer. Data are expressed as means ± standard error and compared using unpaired *t* tests unless otherwise stated. In NTG hearts Iso had pronounced positive inotropic and lusitropic effects, as indicated by an increase in the maximum rates of rise (dP/dt_{max}) and fall (dP/dt_{min}) of the LV pressure trace, respectively. For example, at 25 μl balloon volume, Iso increased LV dP/dt_{max} from 7663 ± 1019 to 14860 ± 1524 mmHg s^{-1} ($P < 0.05$) and LV dP/dt_{min} from −5812 ± 768 to −9997 ± 695 mmHg s^{-1} ($P < 0.05$). The facilitated relaxation was also apparent as a reduction in minimum diastolic pressure (min DP) at all LV volumes ($P < 0.05$ by repeated measures ANOVA). In contrast, in TG hearts, Iso had no significant effect on LV dP/dt_{min}: −4890 ± 682 and −7084 ± 1022 mmHg s^{-1} for control and Iso, respectively, at 25 μl balloon volume) or on the min DP–volume relationship ($P > 0.05$ by repeated measures ANOVA). Furthermore, end-diastolic pressure was significantly greater in TG compared with NTG hearts in the presence of Iso (e.g. a difference of 12 mmHg at 25 μl volume, $P < 0.05$). Surprisingly, although Iso also increased LV dP/dt_{max} in TG hearts (i.e. from 7563 ± 1045 to 12 146 ± 1865 mmHg s^{-1} at 25 μl balloon volume, $P < 0.05$), the positive inotropic effect appeared to be blunted compared with the response in NTG hearts. These results indicate that phosphorylation of cardiac Tn-I is essential for both the relaxant response and increased diastolic compliance induced by Iso in the mouse heart. The unexpected blunting of the inotropic effect of Iso in TG hearts may be secondary to impairment of relaxation and diastolic responses.

This work was supported by the British Heart Foundation.

All procedures accord with current UK legislation.

Intracellular pH, H^+ buffering capacity and H^+ extrusion in isolated myocytes from guinea-pigs with left ventricular hypertrophy induced by thoracic-aortic constriction

C.H. Fry, D.J. Sheridan* and R.P. Gray

*Institute of Urology & Nephrology, University College London and *Academic Cardiology Unit, St Mary's Hospital, Imperial College London, UK*

Left ventricular hypertrophy (LVH) is accompanied by a rise of $[Na^+]_i$ (Gray *et al.* 2001) and a decline of pH_i (Wallis *et al.* 1997). The possibility that alteration of Na^+–H^+ exchange activity is involved in these changes was investigated by measuring the rate of pH recovery after intracellular acidosis.

LVH was induced in guinea-pigs by placing a plastic clip (2 mm diameter) around the ascending aorta under anaesthesia (0.22 ml kg^{-1} sodium pentobarbitone, followed by 49 %–49 %–2 %, N_2O–O_2–halothane mixture inhalation). Sham-operated and unoperated animals served as controls. After 40–100 days the heart was removed after humane killing and heart-to-body-weight ratio (HBR) recorded and myocytes isolated (Hall & Fry, 1992). pH_i was measured in myocytes from the left ventricle (septum and free wall) by incubation with BCECF-AM (2′,7′-bis(carboxyethyl)-5-carboxyfluorescein; 5 μM, 30 min) using epifluorescence microscopy. Myocytes were superfused with Hepes-buffered Tyrode solution at 37°C. Intracellular H^+ buffering capacity (β_i) was estimated by addition and removal of 10 mM NH_4Cl in the presence of 1 mM amiloride as the ratio of $\Delta[NH_4^+]/\Delta pH_i$ on NH_4Cl removal. The rate of pH recovery, $\Delta pH_i/dt$, on NH_4Cl removal in the absence of amiloride was measured and acid efflux rate calculated as the product of β_i ($\Delta pH_i/dt$) between 30 and 150 s after the peak acidosis. Results are means ± S.D. and statistical significance assessed using Student's *t* tests.

Mean pH_i was lower in myocytes from aortic constricted (AC) hearts (6.95 ± 0.08 pH units, $n = 37$) compared with myocytes from unoperated (7.22 ± 0.12, $n = 89$) or sham-operated hearts (7.20 ± 0.12, $n = 37$) ($P < 0.001$). There was a significant negative relationship between pH_i and HBR ($r = -0.715$, $P < 0.001$). β_i was significantly increased in myocytes from AC hearts (104.2 ± 25.5 mequiv l^{-1} pH $unit^{-1}$, $n = 19$ *vs.* 30.5 ± 15.1, $n = 75$, $P < 0.001$) and was related to increasing HBR ($r = 0.625$, $P < 0.001$). β_i increased as steady-state pH_i fell ($r = -0.80$, $P < 0.001$). $\Delta pH_i/dt$ was slower in myocytes from AC hearts ($\tau = 231 \pm 82$, $n = 26$, *vs.* 165 ± 88 s, $n = 88$, $P < 0.001$) but the net acid efflux was not significantly different in the two groups (4.2 ± 1.9, $n = 21$ *vs.* 3.7 ± 1.9 mequiv l^{-1} min^{-1}, $n = 68$, $P > 0.05$).

LVH is accompanied by a decline in pH_i and an increase in sarcoplasmic H^+ buffering capacity, which is pH_i dependent. The recovery from intracellular acidosis is slowed in LVH but the H^+ extrusion rate is unchanged, suggesting that Na^+–H^+ exchange activity is not altered in this model of hypertrophy.

Gray, R.P. *et al.* (2001). *Pflügers Arch.* **442**, 117–123.
Hall, S.K. & Fry, C.H. (1992). *Am. J. Physiol.* **263**, H622–633.
Wallis, W.R. *et al.* (1997). *Exp. Physiol.* **82**, 227–230.

We thank the British Heart Foundation for financial assistance.

All procedures accord with current UK legislation.

Laminin potentiates the contractile response to β-adrenergic, but not endothelin-1, stimulation in rat ventricular myocytes

S.S. Ansari, H.A. Shiels, S.C. Calaghan and E. White

School of Biomedical Sciences, University of Leeds, Leeds LS2 9JT, UK

Binding of the extracellular matrix protein laminin to integrin receptors may modulate intracellular signalling pathways in the heart. We were interested in the effect of laminin on the contractile response of single ventricular myocytes to β-adrenergic and endothelin-1 (ET-1) stimulation.

Male Wistar rats were killed by Schedule 1 procedures. Single ventricular myocytes were isolated by enzymatic digestion and then placed on glass coverslips either in the absence (CON) or presence (LAM) of laminin (final concentration 10 mg ml^{-1}). After at least 2 h of incubation, coverslips were placed in a superfused experimental chamber on an inverted microscope and cell shortening was measured by video edge detection during field stimulation at 0.5 Hz (22–24 °C).

The non-selective β-adrenoreceptor agonist isoprenaline (10^{-8} M) caused a greater increase in shortening in LAM than CON cells ($P < 0.05$, Student's unpaired t test). When β_1-adrenoreceptors were antagonised with 10^{-6} M atenolol, the response to isoprenaline was not different in LAM cells, but almost abolished in CON cells ($P < 0.05$; denoted by dissimilar letters in Fig. 1). By contrast, laminin binding had no significant effect on the inotropic response to 10^{-7}, 10^{-8} or 10^{-9} M ET-1 ($P > 0.05$; Fig. 1, only data for 10^{-8} M shown).

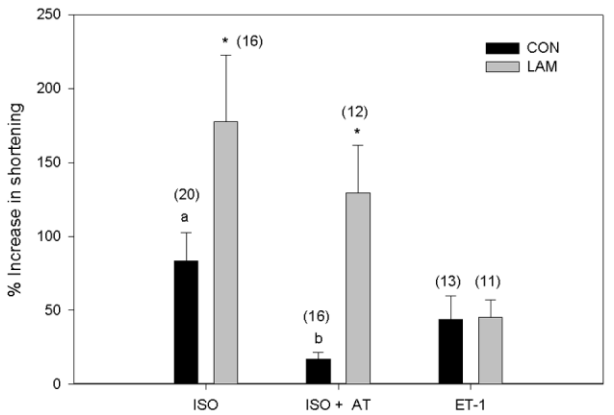

Figure 1. Percentage increase in cell shortening in control and laminin-treated cells in response to isoprenaline (ISO, 10^{-8} M), isoprenaline (10^{-8} M) and atenolol (AT, 10^{-6} M) and endothelin-1 (ET-1, 10^{-8} M). Effects of LAM on response to ISO and ISO + AT were significant as indicated by the *, but response to ET-1 was not altered. Dissimilar letters indicate reduction in control shortening after β_1-adrenoreceptor blockage. The n value for each experiment is given in parentheses.

The effect of laminin on the contractile response to β-adrenergic stimulation in rat ventricular myocytes is consistent with the response of the L-type Ca^{2+} current seen in cat atrial myocytes (Wang *et al.* 2000). This suggests a common mechanism in myocardium that may involve the depression of β_1-adrenergic pathway and stimulation of the β_2-adrenergic pathway. Given the lack of effect of laminin on the response to ET-1, it appears that the impact of laminin is specific for certain signalling pathways.

Wang, Y.G. *et al.* (2000). *J. Physiol.* **527**, 3–9.

This work was supported by the University of Leeds (S.S.A.), the British Heart Foundation (S.C.C.) and the National Science and Engineering Research Council of Canada (H.A.S.).

All procedures accord with current UK legislation.

Heterogeneity in positive inotropic responses of rat ventricular myocytes to endothelin-1

Stephanie C.M. Choisy*, Nicholas S. Freestone† and Andrew F. James*†

**Department of Physiology and Cardiovascular Research Laboratories, School of Medical Sciences, University of Bristol, University Walk, Bristol BS8 1TD and †Cardiac Physiology, St Thomas' Hospital, King's College London, London SE1 7EH, UK*

Endothelin-1 (ET-1), a peptide hormone best known for its vasoconstrictor action, also produces a potent positive inotropic effect and is suggested to contribute to myocardial contractility in a number of species, including man. However, the mechanism of this positive inotropic action remains unclear. We have previously shown in rat ventricular myocytes that ET-1 inhibits a steady-state background K^+ current, an effect that may contribute to its positive inotropic action through prolongation of the action potential duration (APD) (James *et al.* 2001). As part of our investigations into the positive inotropic effect of the peptide hormone, we have examined heterogeneity in the response to ET-1 of rat ventricular myocytes.

Ventricular myocytes were isolated enzymatically from hearts excised under pentobarbitone anaesthesia (150 mg kg^{-1} I.P.) from adult male Wistar rats according to the UK legislation. Myocytes were superfused with Tyrode solution at 35 °C (pH 7.35) and field-stimulated at 0.3 Hz. Myocyte images were acquired via a CCD camera and cell length measured in real-time by edge-detection. The responses to ET-1 were analysed from the average of 20 traces in the absence and presence of the peptide hormone at steady-state. Data are expressed as means ± S.E.M. and analysed by Student's paired and unpaired t tests. ET-1 (1 nM) increased cell shortening by 91.4 ± 11.5 % from 4.7 ± 0.3 to 8.5 ± 0.6 μm ($n = 37$; $P < 0.001$). ET-1 also increased the maximum rate of shortening by 85.6 ± 9.6 % from 115.9 ± 7.3 to 203.0 ± 13.2 μm s^{-1} ($n = 37$; $P < 0.001$) and increased the t_{half} of relaxation by 8.2 ± 2.6 % from 36.9 ± 1.5 ms to 39.3 ± 1.4 ms ($n = 37$; $P < 0.05$). There was a notable degree of variability between cells in responses to ET-1, the increase in cell shortening ranging from 4.8 to 360.9 %. It is well known that the APD varies across the left ventricular free wall due to differences in K^+ current density and this has been suggested to produce heterogeneity in Ca^{2+} influx (Volk *et al.* 1999). Therefore, the effects of ET-1 were investigated on myocytes isolated from the endocardial and epicardial regions. The mean increase in cell shortening was significantly larger in epicardial (3.5 ± 0.4 μm; $n = 11$) than endocardial cells (2.2 ± 0.5 μm; $n = 12$; $P < 0.05$), but this difference was not statistically significant.

Further studies are required to establish the mechanism of action of ET-1 and the basis to the large inter-cell variability in response to the hormone.

James, A.F. *et al.* (2001). *Biochem. Biophys. Res. Comm.* **284**, 1048–1055.
Volk, T. *et al.* (1999). *J. Physiol.* **519**, 841–850.

This work is kindly supported by the British Heart Foundation.

All procedures accord with current UK legislation.

Triphosphate is an effective activator of the sheep cardiac ryanodine receptor

M. Sitsapesan*, W.M. Chan*, W. Welch† and R. Sitsapesan*

*Department of Pharmacology, University of Bristol, University Walk, Bristol BS8 1TD and †University of Nevada School of Medcine, Reno, Nevada, NV 89557, USA

ATP and related adenine nucleotides are thought to play an important regulatory role as activators of the cardiac ryanodine receptor (RyR). We have previously demonstrated that the phosphate groups of ATP provide most of the energy required to activate the channel (Chan *et al.* 2000) but it has been assumed that the adenine moiety of ATP is essential for recognition and binding to the adenine nucleotide site. To examine if the triphosphate group requires the adenine (and ribose) group for activity at the cardiac RyR we have therefore investigated if triphosphate (PPPi) alone can activate cardiac RyR channels.

Native RyR from sheep hearts obtained from an abattoir were incorporated into bilayers under voltage-clamp conditions and single-channel recordings were monitored with Ca^{2+} as the permeant ion as previously described (Chan *et al.* 2000). [^{3}H]ryanodine binding to isolated heavy SR was performed as previously described (Kermode *et al.* 1998). In the presence of 10 μM Ca, the amount of [^{3}H]ryanodine bound to the heavy SR membrane fraction was 0.232 ± 0.020 pmol (mg protein)$^{-1}$ (mean ± S.D.; $n = 3$). ATP (10 mM), PPPi (10 mM), adenosine (5 mM), pyrophosphate (PPi) (10 mM) and inorganic phosphate (Pi) (10 mM) stimulated ryanodine binding to 163, 140, 112, 102 and 108 % of control, respectively ($n = 3$). In agreement with the binding studies, the open probability (P_o) of single RyR channels incorporated into bilayers was increased in a concentration-dependent manner by PPPi. For example, in a typical channel, P_o was 0.059 in the presence of 10 μM cytosolic Ca^{2+} alone and was 0.126 and 0.66 after cytosolic addition of 1 and 10 mM PPPi, respectively.

In summary we have shown that PPPi can activate the cardiac RyR but not as effectively as ATP. The adenine moiety is therefore not essential for activation of the channel but is required to realise the full activating potential of the PPPi group.

Chan, W.M. *et al.* (2000). *Br. J. Pharmacol.* **130**, 1618–1626.

Kermode, H. *et al.* (1998). *FEBS Lett.* **431**, 59–62.

This work was supported by the British Heart Foundation.

Inhibition of cardiac and skeletal ryanodine receptors by the polyunsaturated fatty acid eicosapentaenoic acid (EPA)

J.S. Swan*, S.C. O'Neill† and Rebecca Sitsapesan*

*Department of Pharmacology, University of Bristol, Medical School, University Walk, Bristol BS8 1TD, UK and †Department of Medicine, University of Manchester, Manchester M13 9PT, UK

Experimental evidence indicates that polyunsaturated fatty acids (PUFAs) have a protective effect against ischaemia-induced arrhythmias when present in the diet (Leaf *et al.* 1999). More recently, it has been shown that two PUFAs, eicosapentaenoic acid (EPA) and docosahexaenoic acid (DHA), reduce the frequency of the potentially arrhythmogenic spontaneous waves of Ca^{2+} release in isolated cardiac cells (Negretti *et al.* 2000) and part of this action appears to result from an inhibitory effect on sarcoplasmic reticulum (SR) Ca^{2+} release.

To identify a possible mechanism for the inhibition of SR calcium release, we examined the effects of the n-3 PUFA eicosapentaenoic acid (EPA) on the gating properties of native ryanodine receptors (RyR). Pig skeletal and sheep cardiac muscle was obtained from an abattoir. Native sheep cardiac or pig skeletal RyR were incorporated into planar phospholipid bilayers under voltage-clamp conditions and single-channel current fluctuations were monitored at 0 mV with Ca^{2+} as the permeant ion as described previously (Chan *et al.* 2000).

In the presence of 1 mM ATP and 1 μM free cytosolic Ca^{2+}, cardiac RyR open probability (P_o) was 0.65 ± 0.08 ($n = 3$). With the addition of 10, 20 and 100 μM EPA to the cytosolic channel side, the P_o was 0.52 ± 0.25, 0.34 ± 0.17 and 0.20 ± 0.08, respectively (mean ± S.D.; $n = 3$), demonstrating a dose-dependent inhibitory effect. Under identical experimental conditions, EPA exerted similar effects on the skeletal RyR: control P_o was 0.47 ± 0.25 and 0.36 ± 0.29, 0.3 ± 0.32 and 0.11 ± 0.08 with the addition of 10, 20 and 100 μM EPA, respectively (mean ± S.D.; $n = 7$). The effect of EPA on RyR P_o is therefore not isoform specific.

The inhibitory action of EPA results from both a decrease in mean open times and a reduction in the frequency of channel opening. Control mean open and closed times were 7.02 ± 6.17 and 2.26 ± 1.05 ms^{-1}, respectively, and were 1.94 ± 1.8 and 27.54 ± 44.12 ms^{-1}, respectively, in the presence of 10 μM EPA (mean ± S.D.; $n = 3$).

These results demonstrate that EPA reduces RyR P_o in a dose-dependent manner and at concentrations that could be achieved with supplementation of the diet with fish oils (Negretti *et al.* 2000). The inhibitory effect of EPA on RyR channel gating is a possible mechanism to explain the inhibition of SR Ca^{2+} release in cardiac cells by PUFAs and may contribute to their anti-arrhythmic properties.

Chan, W.M. *et al.* (2000). *Br. J. Pharmacol.* **130**, 1618–1626.

Leaf, A. *et al.* (1999). *J. Memb. Biol.* **172**, 1–11.

Negretti, N. *et al.* (2000). *J. Physiol.* **523**, 367–375.

This work was supported by the British Heart Foundation.

The effects of calmodulin on the sheep cardiac ryanodine receptor

Adam Hill* and Rebecca Sitsapesan†

*NHLI, Imperial College, London and †Department of Pharmacology, University of Bristol, Bristol, UK

Calmodulin (CaM) has been shown to reduce the open probability (P_o) of skeletal ryanodine receptor (RyR) channels in the presence of micromolar cytosolic Ca^{2+} but increase P_o at nanomolar levels of cytosolic Ca^{2+}. It has been suggested that suramin modifies RyR function by interacting with CaM binding sites on RyR (Klinger *et al.* 1999). In the present study we have examined the effects of calmodulin on the sheep cardiac RyR and investigated the possibility that suramin and calmodulin act via the same binding sites. Sarcoplasmic reticulum (SR) membrane vesicles were isolated as described previously (Kermode *et al.* 1998) from sheep hearts obtained from an abattoir and were either incorporated into artificial membranes for single-channel studies or were used for [^{3}H]ryanodine binding or Western blotting (Kermode *et al.* 1998).

In the presence of 100 μM cytosolic free Ca^{2+}, 50 nM CaM reduced the P_o of RyR from 0.314 ± 0.082 to 0.031 ± 0.02 (S.E.M.;

$n = 5$). At this same [Ca^{2+}], CaM dose-dependently inhibited [^{3}H]ryanodine binding to isolated SR vesicles (35 ± 3 % reduction at 5 μM CaM (S.E.M.; $n = 4$)), while CaM had no effect on binding at nanomolar Ca^{2+} ($n = 3$). In contrast to the apparently simple inhibitory effect of CaM in the presence of 100 μM Ca^{2+}, suramin exerts a triphasic effect on cardiac RyR gating. Nanomolar concentrations of suramin inhibit [^{3}H]ryanodine binding (25 ± 9 % reduction at 100 nM); micromolar suramin stimulates binding (23 ± 5 % increase at 100 μM suramin) and millimolar suramin inhibits binding (58 ± 4 % reduction at 2 mM suramin) (S.E.M.; $n = 4$). Western blotting was used to investigate if the two ligands compete for the same binding sites on RyR. SR vesicles were incubated with suramin to investigate if suramin could displace endogenously bound CaM from RyR. SR vesicles were then sedimented and the pellet and supernatant were run on a 10 % acrylamide gel and blotted with anti-CaM antibodies (Upstate Biotech, Bucks). In all cases CaM remained associated with the RyR channel protein, providing no evidence that it could be competitively displaced by suramin.

Our results demonstrate that CaM reduces the P_o of cardiac RyR channels in the presence of 100 μM Ca^{2+}, but although suramin can also reduce P_o at certain concentrations we find no compelling evidence to suggest that the two ligands decrease P_o by binding to the same sites on RyR.

Kermode, H. *et al.* (1998). *FEBS Lett.* **431**, 59–62.

Klinger, M. *et al.* (1999). *Mol. Pharmacol.* **55**, 462–472.

This work was supported by the BHF.

Investigation of the role of sodium–calcium exchange in cardiac pacemaking in the guinea-pig sino-atrial node

M.J. Lowe, T. Salter, S. Rakovic and D.A. Terrar

Department of Pharmacology, University of Oxford, Mansfield Road, Oxford OX1 3QT, UK.

It has recently been suggested that sodium–calcium exchange current ($I_{Na\text{-}Ca}$) may be involved in cardiac pacemaking, for example by contributing to the end of the pacemaker depolarisation in cat sino-atrial (SA) node cells (Huser *et al.* 2000). The aim of this study was to investigate the possible role of $I_{Na\text{-}Ca}$ in pacemaking in guinea-pig SA node cells.

Male guinea-pigs were killed by cervical dislocation following stunning. Beating rate was measured either in atrial preparations with an intact SA node, or in single SA node cells isolated enzymatically from the heart. Calcium transients in single SA node cells were measured using either confocal microscopy (cells loaded with 3 μM fluo-4 AM for 10 min), or conventional fluorescence microscopy (1.5 μM indo-1 AM, 10 min). $I_{Na\text{-}Ca}$ was inhibited by reducing the Na^+ concentration of the superfusion solution (2.5 mM Ca^{2+}, 36 °C) from 133 to 73.75 mM (Li^{2+} as the substitute). Data are quoted as means ± S.E.M. and statistical significance assessed using Student's paired *t* test.

In the absence of other drugs, switching to a low Na^+ solution caused a decrease in beating rate of 16 ± 2 % in atrial preparations ($P < 0.05$, $n = 5$), and 35 ± 5 % in single SA node cells ($P < 0.05$, $n = 5$). In SA node cells imaged using confocal microscopy, the rate of generation of spontaneous calcium transients was reduced by 14 ± 4 %, calcium transient amplitude (F/F_0) was increased by 91 ± 22 %, and calcium transient duration was increased as a result of a 50 ± 14 % lengthening in the time to peak (all after 1 min in low Na^+ solution, $P < 0.05$, $n = 4$); there was no significant change in the time for decay of the calcium transient to 50 % of its peak. In three of these four cells, there was also an increase in the minimum diastolic calcium level.

In the presence of 100 nM isoprenaline, switching to a low Na^+ solution caused a 41 ± 1 % decrease in beating rate in atrial preparations ($P < 0.05$, $n = 3$). In single SA node cells, switching to low Na^+ in the presence of 100 nM isoprenaline reduced the rate of generation of spontaneous calcium transients (measured using indo-1) by 17 ± 3 %, increased calcium transient amplitude by 24 ± 7 %, and lengthened time to peak by 34 ± 11 % ($P < 0.05$, $n = 6$) with no significant change in the time taken for 50 % decay. The minimum diastolic calcium level was increased by 11 ± 3 % ($P < 0.05$, $n = 6$).

These data are consistent with a role for $I_{Na\text{-}Ca}$ in the pacemaker depolarisation of guinea-pig SA node cells. It remains to be determined how changes in calcium transient characteristics and in minimum diastolic calcium levels contribute to the regulation of pacemaker rate.

Huser, J. *et al.* (2000). *J. Physiol.* **524**, 415–422.

This work was supported by BHF and The Wellcome Trust.

All procedures accord with current UK legislation.

Inhibition of changes in calcium transients and left ventricular inotropy with sympathetic stimulation in the presence of background vagal stimulation – studies in the isolated, innervated rabbit heart

K.E. Brack*, J.H. Coote* and G.A. Ng†

**Department of Physiology, University of Birmingham, Birmingham and †Division of Cardiology, University of Leicester, Glenfield Hospital, Leicester, UK*

Cellular and pharmacological studies have shown that the positive inotropic effect with adrenergic stimulation is mediated by changes in Ca^{2+} homeostasis. The effects of direct autonomic nerve stimulation on Ca^{2+} transients (CaT) have not been investigated in the whole heart. It was the aim of this study to examine (1) the changes in CaT and left ventricular (LV) inotropy with sympathetic stimulation (SS) and (2) the effects of background vagal stimulation (VS) on these changes, in the isolated heart with intact dual autonomic innervation.

Adult male NZW rabbits (2.4 ± 0.1 kg, mean ± S.E.M., $n = 8$) were humanely killed with an overdose of I.V. Sagatal. Hearts were isolated and the thoracic spine with sympathetic outflow preserved with both vagus nerves isolated at the mid-cervical region. The preparation was perfused with Tyrode solution (37 °C) in constant flow Langendorff mode via the ascending aorta and loaded with fura-2 AM. After washout, epicardial fluorescence (F) from the LV free wall was measured at 510 nm for excitation wavelengths 340 ± 13 and 380 ± 10 nm and CaT was measured as the F_{340}/F_{380} ratio. LV pressure (LVP) was measured via an intraventricular balloon. Measurements were made at steady state (right ventricular pacing, 250 b.p.m.) during (1) SS at 2 [low], 5 [med] and 10 [high] Hz, and (2) high SS with background bilateral VS at 20 Hz (VS/SS High), and analysed using ANOVA.

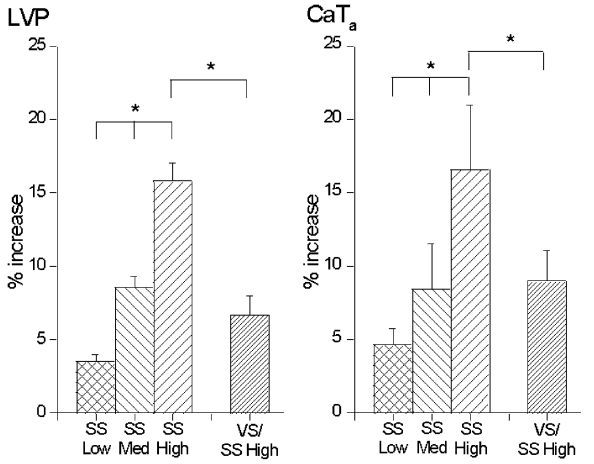

Figure 1. Per cent change in LVP and CaT_a.

Table 1. Effect of SS and VS on LVP and CaT

	LVP (mmHg)	dP/dT^+ (mmHg ms^{-1})	dP/dT^- (mmHg ms^{-1})
Baseline	34.2 ± 2.4	0.52 ± 0.06	-0.43 ± 0.05
SS Low	35.5 ± 2.5	0.55 ± 0.06	-0.46 ± 0.05
SS Med	36.6 ± 2.5	0.60 ± 0.07	-0.48 ± 0.05
SS High	39.5 ± 3.0	0.70 ± 0.09	-0.53 ± 0.06
VS/SS High	35.5 ± 2.6†	0.59 ± 0.08†	-0.46 ± 0.06†
	CaT_d	CaT_s	CaT_a
Baseline	1.054 ± 0.023	1.104 ± 0.019	0.049 ± 0.005
SS Low	1.053 ± 0.023	1.105 ± 0.019	0.051 ± 0.005
SS Med	1.054 ± 0.023	1.107 ± 0.019	0.052 ± 0.005
SS High	1.054 ± 0.023	1.110 ± 0.019	0.055 ± 0.006
VS/SS High	1.052 ± 0.023†	1.103 ± 0.019†	0.052 ± 0.005†

†$P < 0.05$ compared with SS High.

The results are as follows. (1) SS resulted in a frequency-dependent increase ($P < 0.05$) in LVP, dP/dT^+ and dP/dT^- (see Table 1). Diastolic level of CaT (CaT_d) was unchanged during SS whilst peak systolic level of CaT (CaT_s) and CaT amplitude (CaT_a) was increased in a frequency-dependent manner ($P < 0.05$). (2) Background VS inhibited the changes ($P < 0.05$) in LV inotropy and CaT with SS (see Fig. 1 and Table 1).

In conclusion, sympathetic nerve stimulation increased systolic Ca^{2+} and Ca^{2+} transient amplitude in the isolated, innervated rabbit heart in a frequency-dependent manner, in line with inotropic changes. These changes were inhibited in the presence of background vagus nerve stimulation.

This work was supported by a British Heart Foundation grant.

All procedures accord with current UK legislation.

Intracellular Ca^{2+} regulation in isolated myocytes from guinea-pigs with left ventricular hypertrophy induced by constriction of the thoracic aorta

R.P. Gray, D.J. Sheridan* and C.H. Fry

*Institute of Urology & Nephrology, University College London and *Academic Cardiology Unit, St Mary's Hospital, Imperial College London, UK*

Left ventricular hypertrophy (LVH) is accompanied by a rise of $[Na^+]_i$, the mechanism of which is unclear (Gray *et al.* 2001). A primary increase of $[Ca^{2+}]_i$ would, via Na^+–Ca^{2+} exchange, lead to an increase of $[Na^+]_i$. The possibility that in LVH the ability of the myocyte to regulate sarcoplasmic Ca^{2+} as a result of reduced sarcoplasmic reticulum (SR) function was investigated.

LVH was induced by placing a plastic clip (2 mm diameter) around the ascending aorta under anaesthesia (0.22 ml kg^{-1} sodium pentobarbitone, followed by 49 %–49 %–2 %, N_2O–O_2–halothane mixture inhalation). Sham-operated and unoperated animals served as controls. After 40–100 days the heart was removed from humanely killed animals and the heart-to body weight ratio (HBR) recorded; myocytes were isolated as described previously (Hall & Fry, 1992). Intracellular $[Ca^{2+}]$ was measured using epifluorescence microscopy using fura-2 AM (5 μM, 30 min incubation). Myocytes were superfused with HCO_3^-/CO_2-buffered Tyrode solution at 37°C. To estimate the SR Ca^{2+} content, the rise of $[Ca^{2+}]_i$ when released by 10 mM caffeine was recorded. Ca^{2+} efflux rate was estimated from the time constant (τ_1) of decay of the caffeine response (Varro *et al.* 1993). Results are expressed as means ± S.D. and statistical significance assessed using Student's *t* test.

Caffeine (10 mM) generated a Ca^{2+} transient in all cells ($n = 74$) from control hearts and in 40 of 46 cells from AC hearts. The magnitude of the transient was on average 55 % in the AC group compared with control ($P < 0.01$). τ_1 was slower in myocytes from AC hearts (15.0 ± 5.5, $n = 40$, *vs.* 9.7 ± 3.9 s, $n = 46$, $P < 0.001$) and correlated with HBR ($r = 0.57$, $P < 0.01$). A transient undershoot of $[Ca^{2+}]_i$ was observed in a number of myocytes on removal of caffeine and the time constant of this was prolonged in myocytes from AC hearts (71.2 ± 33.9, $n = 24$ *vs.* 51.8 ± 16.3 s, $n = 16$, $P < 0.05$) and also correlated with HBR ($r = 0.73$, $P < 0.01$). Reduction of extracellular [Na] from 147 to 29 mM increased $[Ca^{2+}]_i$ by a similar magnitude in myocytes from AC and control hearts (604 ± 716, $n = 39$ *vs.* 540 ± 591 nM, $n = 64$, $P > 0.05$). τ_1 in myocytes from control and AC hearts were prolonged compared with those in 147 mM Na^+ Tyrode (10.0 ± 3.9 *vs.* 17.3 ± 10.3 s, $n = 27$, $P < 0.001$ for control and 15.1 ± 5.7 *vs.* 19.4 ± 9.6 s, $n = 17$, $P < 0.05$ for aortic constricted group, paired *t* tests).

These findings suggest that SR Ca^{2+} regulation is impaired in this model of LVH and that Na^+–Ca^{2+} exchange activity is also modulated.

Gray, R.P. *et al.* (2001). *Pflügers Arch.* **442**, 117–123.

Hall, S.K. & Fry, C.H. (1992). *Am. J. Physiol.* **263**, H622–633.

Varro, A. *et al.* (1993). *Pflügers Arch.* **423**, 158–160.

We thank the British Heart Foundation for financial assistance.

All procedures accord with current UK legislation.

Electrophysiological properties of the L-type Ca^{2+} current in cardiomyocytes from Pacific mackerel and bluefin tuna

H.A. Shiels*, J.M. Blank†, A.P. Farrell‡ and B.A. Block†

**School of Biomedical Sciences, University of Leeds, Leeds, UK, †Hopkins Marine Station, Stanford University, CA, USA and ‡Department of Biological Sciences, Simon Fraser University, Burnaby, BC, Canada*

Among active fish species, tunas are renowned for high maximum heart rates and high cardiac output (Farrell, 1991). The greater contractile strength and maximum heart rate of tunas suggest that Ca^{2+} delivery via either trans-sarcolemmal or sarcoplasmic reticulum pathways may be enhanced in tuna myocytes compared with other fish. In this study, we investigated the properties of the L-type Ca^{2+} channel current (I_{Ca}) to test the hypothesis that Ca^{2+} influx would be larger and have faster kinetics in myocytes from bluefin tuna (*Thunnus thynnus*) compared with those of its sister taxa the Pacific mackerel (*Scomber japonicus*).

Bluefin tuna and Pacific mackerel were humanely killed by cervical dislocation, the hearts were removed and atrial and ventricular myocytes were isolated by enzymatic digestion. Myocytes were whole-cell voltage-clamped and the electrophysiological properties of I_{Ca} were examined at 20 ± 1 °C, which was the acclimation temperature of the fish. All values are given as means ± S.E.M. and differences between species were considered significant at $P < 0.05$ using Student's unpaired *t* tests.

Atrial myocytes from bluefin tuna had a greater peak current amplitude (-4.8 ± 0.3 pA pF^{-1}; $n = 32$ cells) compared with those from mackerel (-2.7 ± 0.5 pA pF^{-1}; $n = 12$ cells). We observed faster fast inactivation kinetics in tuna atrial myocytes compared with mackerel atrial myocytes ($\tau_f = 25.9 \pm 1.6$ *vs.* 33.6 ± 3.9 ms, respectively) and the slope (k) of steady-state activation and inactivation was greater in tuna (activation, $k = 6.19 \pm 0.1$; inactivation, $k = 5.29 \pm 0.3$) compared with mackerel (activation, $k = 7.69 \pm 0.7$; inactivation, $k = 9.31 \pm 0.5$).

In contrast to atrial myocytes, ventricular myocytes did not differ between species in terms of current density and inactivation kinetics. However, I_{Ca} for tuna ventricular myocytes activated at significantly more depolarized voltages (tuna, -10.6 ± 0.6 mV, $n = 19$; mackerel, -14.3 ± 1.0 mV, $n = 22$).

Our results indicate that atrial myocytes of bluefin tuna have significantly enhanced Ca^{2+} flux pathways in comparison with those of Pacific mackerel. This supports the hypothesis that distinct differences do exist between bluefin tuna and Pacific mackerel, which may be associated with the elevated maximal heart rates observed in tuna. However, further studies are necessary to confirm this possibility, as well as to explain why ventricle myocytes did not show similar differences.

Farrell, A.P. (1991). *Physiol. Zool.* **64**, 1137–1164.

This research is supported by NSERC to A.P.F. and H.A.S. and the Monterey Bay Aquarium Foundation to B.A.B.

All procedures accord with current National and local guidelines.

Actions of 17β-oestradiol on the current–voltage relationship for the L-type calcium current (I_{Ca}) in ventricular myocytes isolated from male and female rats

K.L. Philp*†, S.J. Coker*, M. Hussain† and G. Hart†

*Departments of *Pharmacology & Therapeutics and †Medicine, University of Liverpool, Liverpool L16 3GA, UK*

17β-Oestradiol is anti-arrhythmic in female rats subjected to myocardial ischaemia (Philp *et al.* 2001). 17β-Oestradiol inhibits I_{Ca} in female ventricular myocytes (Meyer *et al.* 1998), although the actions of 17β-oestradiol in male myocytes are unknown. Male blood vessels do not respond in the same manner as female vessels to oestrogen supplementation (McNeill *et al.* 1996), suggesting a gender-dependent action of oestrogen. If 17β-oestradiol reduces the current–voltage (I–V) relationship for I_{Ca} in a gender-dependent manner, this may account for the anti-arrhythmic effects observed in female rats, as Ca^{2+} channel blockade is anti-arrhythmic in rats (Curtis *et al.* 1987). Therefore, we have investigated the effects of 0.1 μM 17β-oestradiol on the I–V relationship for I_{Ca} in male and female ventricular myocytes.

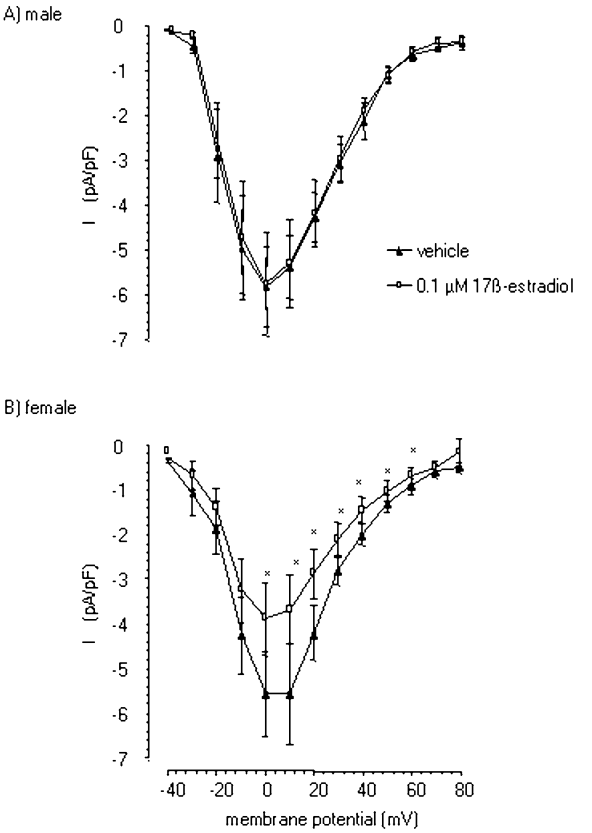

Figure 1. Effects of 0.1 μM 17β-oestradiol on the I–V relationship for I_{Ca} in male (A) and female (B) rat ventricular myocytes. *$P < 0.05$ *vs.* vehicle.

Wistar rats (250–320 g) were humanely killed by Schedule 1 procedures. Ventricular myocytes were isolated by enzymatic digestion. I–V curves were constructed using the whole-cell patch-clamp technique. External solutions contained (mM): NaCl, 140; KCl, 5.4; $MgCl_2$, 1; $CaCl_2$, 1; glucose, 10; Hepes, 10; pH 7.35 with TEAOH. Internal pipette solution contained: caesium glutamate, 120; KCl, 20; $MgCl_2$, 5; Na_2-ATP, 5; EGTA, 1; Hepes, 10; pH 7.2 with CsOH. Cells were held at −40 mV and depolarized to +80 mV in 10 mV steps at 0.5 Hz. Cells were exposed to 0.2 % ethanol in normal Tyrode (vehicle) for 3 min

and then to 17β-oestradiol (0.1 μM) for a further 3 min to determine the effect of 17β-oestradiol. All recordings were performed at 35°C. $n \geqslant 9$ cells per group.

17β-Oestradiol had no significant effect on the *I–V* relationship in myocytes from males (Fig. 1A). In contrast, 0.1 μM 17β-oestradiol significantly reduced the *I–V* curve for I_{Ca} between 0 and +60 mV in female rats (Fig. 1B). Peak I_{Ca} at 0 mV in males were 5.8 ± 0.9 pA pF^{-1} (vehicle), 5.76 ± 1.2 pA pF^{-1} (17β-oestradiol), and in females rats 5.3 ± 1.0 pA pF^{-1} (vehicle), 3.7 ± 0.8 pA pF^{-1} (17β-oestradiol) (mean ± S.E.M., $P < 0.05$, Student's paired *t* test).

In conclusion, we suggest that the increased sensitivity of I_{Ca} to inhibition by 17β-oestradiol in females may underlie the observed gender differences in the anti-arrhythmic action of 17β-oestradiol.

Curtis, M.J. *et al.* (1987). *J. Mol. Cell. Cardiol.* **19**, 399–419.
McNeill, A.M. *et al.* (1996). *Eur. J. Pharmacol.* **308**, 305–309.
Meyer, R. *et al.* (1998). *Exp. Physiol.* **83**, 305–321.
Philp, K.L. *et al.* (2001). *Proc. West. Pharm. Soc.* **44**, p265.

This work was supported by the British Heart Foundation FS/99060.

All procedures accord with current UK legislation.

Effects of halothane on intracellular Ca^{2+} in ventricular myocytes from streptozotocin-induced diabetic rat

A. Rithalia*, M.A. Qureshi†, S.M. Harrison* and F.C. Howarth†

**School of Biomedical Sciences, University of Leeds, Leeds, UK and †Department of Physiology, Faculty of Medicine and Health Sciences, United Arab Emirates University, United Arab Emirates*

Contractile dysfunction has been reported in ventricular myocytes from the streptozotocin (STZ)-induced diabetic rat model, which include a prolonged time course and reduced amplitude of contraction (Ren & Davidoff, 1997; Howarth *et al.* 2000), although the role of intracellular Ca^{2+} regulation in these effects is still unclear. Volatile general anaesthetics (e.g. halothane) in addition to inducing unconsciousness, also have a potent negative inotropic effect on the heart (Davies *et al.* 1999) linked to altered Ca^{2+} regulation. The aim was to investigate the role of altered Ca^{2+} regulation in contractile dysfunction in myocytes from the STZ-induced diabetic rat in the absence and presence of a clinically relevant dose of halothane.

Diabetes was induced in male Wistar rats by I.P. injection of STZ (60 mg kg^{-1}) and animals killed humanely 8–12 weeks following treatment (methodology approved by Faculty of Medicine and Health Sciences Animal Ethics Committee). Characteristics of electrically evoked cytosolic Ca^{2+} transients and caffeine-evoked Ca^{2+} transients, which provide a measure of sarcoplasmic reticulum (SR) Ca^{2+} content, were measured in fura-2-loaded control and STZ myocytes in the absence and presence of 0.6 mM halothane at 35–36°C. Data are expressed as means ± S.E.M. (*n* cells) and statistical comparisons made using either unpaired or paired *t* tests as appropriate.

The amplitude of the electrically evoked Ca^{2+} transient was significantly ($P < 0.001$) reduced (by ~45 %) in STZ compared with control myocytes. The time course of the Ca^{2+} transient was prolonged ($P < 0.001$) following STZ treatment; time to peak was 72 ± 4 ms (30) *vs.* 55 ± 3 ms (34) and time to half-relaxation was 220 ± 9 ms *vs.* 158 ± 8 ms in STZ and control myocytes, respectively. Halothane reduced ($P < 0.001$) Ca^{2+} transient amplitude in both STZ and control myocytes; however, the relative magnitude of this reduction was not different between control and STZ myocytes ($P > 0.05$).

The amplitude of the caffeine-evoked Ca^{2+} transient was not significantly altered by STZ treatment. In control cells, halothane significantly reduced SR Ca^{2+} content by 28 ± 4 % ($P < 0.001$) and the magnitude of this reduction was not significantly different ($P > 0.05$) in STZ myocytes. Fractional SR Ca^{2+} release was increased to a similar extent in both STZ and control myocytes by halothane. These data suggest that altered mechanisms of Ca^{2+} transport might underlie the contractile abnormalities reported in myocytes from STZ-treated rats but these do not appear to be further complicated by halothane.

Davies, L.A. *et al.* (1999). *Brit. J. Anaes.* **82**, 723–730.
Howarth, F.C. *et al.* (2000). *Acta Diabetol.* **37**, 119–124.
Ren, R. & Davidoff, A.J. (1997). *Am. J. Physiol.* **272**, H148–158.

All procedures accord with current local guidelines.

Changes in SR Ca content in response to variable stimulation rates in rat atrial myocytes

A.P. Walden, C.J. Garratt and A.W. Trafford

Unit of Cardiac Physiology, The University of Manchester, Manchester M13 9PT, UK

The sarcoplasmic reticulum acts as the main intracellular store of Ca used to activate contraction within cardiac myocytes. Mechanisms which increase the Ca content of the SR are positively inotropic, although they can also lead to after-depolarisations thought to be involved in arrhythmogenesis.

Electrical remodelling in the atrium occurs in response to prolonged rapid rates of stimulation and leads to an abbreviation of the action potential duration and to self perpetuation of atrial arrhythmias. A reduction of the L-type Ca current has been shown in humans with atrial fibrillation. Calcium overload has also been shown in electrically remodelled atrial cells.

The aim of the current experiments was to determine whether changing the rate of stimulation alters the Ca load of the SR. Cells were isolated from humanely killed male Wistar rats (200–250 g) by a collagenase and protease digestion technique. Cells were voltage clamped using the perforated patch technique and stimulated at rates of 0.25, 0.5 and 1 Hz at 37 °C. Fluorescence measurements were performed using fluo-3. Caffeine (10 mM) was applied to discharge the SR of Ca and the resulting Na–Ca exchange current (Fig. 1A) was integrated (Fig. 1B) to determine SR Ca content.

Results were obtained for $n = 8$ myocytes. SR Ca content, expressed as the integral relative to cell capacitance in pC/pF, was found to be on average 0.81 ± 0.15 at 0.25 Hz, 0.63 ± 0.12 at 0.5 Hz and 0.86 ± 0.14 at 1 Hz (Fig. 1C). Using paired *t* tests, a statistically significant difference was found comparing 0.5 Hz with 0.25 Hz ($P < 0.05$) and 0.5 Hz with 1 Hz ($P < 0.05$), but not comparing 0.25 Hz with 1 Hz. The changes seen in the SR Ca content were mirrored in the systolic Ca transients which were larger at 0.25 and 1 Hz compared with 0.5 Hz. It remains to be seen whether these changes can be accounted for by differences in the L-type Ca current and what changes occur at higher rates.

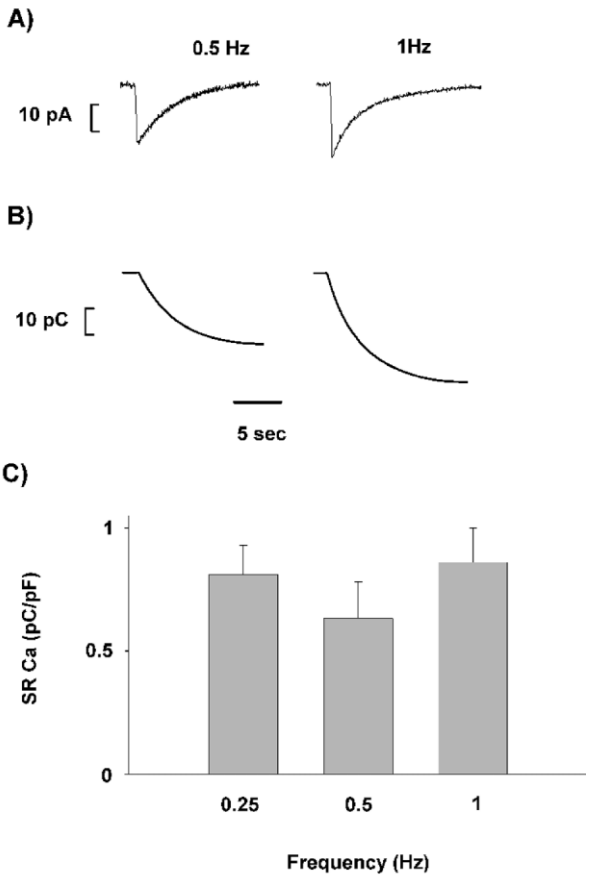

Figure 1. The Na–Ca exchange currents are shown in A showing a smaller current on the left with a stimulation frequency of 0.5 Hz than the right at 1 Hz. This difference is seen more clearly in B where the integrals of the exchange currents have been plotted. C is a histogram of the SR Ca content expressed in pC/pF (see text).

Goette, A. *et al.* (1996). *Circulation* **94**, 2968–2974.
Van Wagoner, D.R. *et al.* (1999). *Circ. Res.* **85**, 428–436.

All procedures accord with current UK legislation.

Comparison of pro-arrhythmic effects of several class III anti-arrhythmic drugs in rabbit Purkinje fibres

L. Sallé, J.-C. Legrand, J. Ducroq, R. Rouet, P. Ducouret and J.-L. Gérard

Laboratoire de Physiologie Cellulaire, Université de Caen, 14032 Caen cedex, France

The aim of this study was to evaluate the pro-arrhythmic effects of class III anti-arrhythmic drugs. We studied pure I_{Kr} (rapid component of delayed rectifier potassium current) blockers (dofetilide and D-sotalol) *versus* pure I_{Ks} (slow component of delayed rectifier potassium current) blockers (chromanol 293B and HMR 1556) in the same preparation. Moreover, we have compared these results with a recent class III agent, azimilide which blocks the two I_{Kdr} (delayed rectifier potassium current) components. We studied the effects of these drugs on the action potential (AP) parameters recorded using the microelectrode technique. The occurrence of early afterdepolarisations (EADs) in the presence or not of adrenaline was also analysed.

Rabbits were humanely killed according to the ethical standards of the French Ministry of Research. Purkinje fibres were dissected and superfused with Tyrode solution. Each drug at different concentrations (from 10^{-9} to 10^{-5} M, $n = 9$ for each agent at each concentration) were added alone during 30 min and then with adrenaline (10^{-8} M) during the following 30 min. Shift of pacing cycle length from 1000 to 2000 ms was done to evaluate the influence of bradycardia on EAD elicitation. Modulations of AP duration are expressed as means ± S.E.M. Statistical analysis of AP parameters was performed using ANOVA followed by a Dunnet's test (intragroup comparison) and an ANOVA for multiple factors (intergroup comparison). Non-parametric factors were compared using an exact Fischer test. $P < 0.05$ was considered as statistically significant.

Pure I_{Kr} blockers and azimilide significantly increased AP duration measured at 90 % of repolarisation (APD_{90}) in a dose-dependent manner. At concentrations inducing similar prolongation of APD_{90} (respectively by 46.3 ± 4.9, 35.4 ± 3.7 and 43 ± 3.7 % for the following drugs), dofetilide (5×10^{-9} M), D-sotalol (10^{-5} M) and azimilide (5×10^{-7} M) promoted EADs respectively in three, six and one cases of nine experiments under adrenergic stimulation. Pure I_{Ks} blockers failed to increase APD_{90} in our conditions and did not induce EADs. Besides, results demonstrated that EAD occurrence is potentiated by bradycardia and adrenergic stimulation.

We concluded that class III anti-arrhythmic drugs that block I_{Kr} showed more pro-arrhythmic effects than those that block I_{Ks}. Azimilide seemed to be the most promising class III compound as it exhibited low pro-arrhythmic effects, despite its ability to lengthen cardiac AP duration, contrary to chromanol 293B and HMR 1556, which failed to increase APD_{90}.

All procedures accord with current National guidelines.

hERG channel blockers prolong guinea-pig cardiomyocyte action potential duration in a concentration-dependent manner

C.S. Davie, C.E. Pollard*, J.-P. Valentin*, J. Mitcheson†, N.B. Standen† and B. Thong

*Lead Generation, AstraZeneca, R&D Charnwood, Loughborough LE11 5RH, *Safety Pharmacology, Safety Assessment, AstraZeneca, Alderley Park SK10 4TJ and †Department of Cell Physiology & Pharmacology, University of Leicester, Leicester LE1 7RH, UK*

Drug-induced prolongation of the QT interval, in humans, is characterised by the block of the rapidly activating voltage-dependent potassium (I_{Kr}) channel, which is the product of the *ether-a-go-go* (ERG) gene. Compounds that cause QT prolongation are currently assessed *in vitro* using hERG cell lines and isolated Purkinje fibre. These methods are not ideal because working on Purkinje fibres gives results very slowly and only one ion channel type can be measured in the hERG cell line. In contrast, myocytes allow the measurement of action potentials (AP) and their underlying ion channels. The aim of this study was to assess and compare the effect of known hERG channel blockers on I_{Kr} and AP duration in guinea-pig myocytes.

Adult guinea-pigs were humanely killed and ventricular myocytes were isolated by enzymatic digestion. The cells were

continuously perfused with Tyrode solution at 33–35 °C containing (mM): 135 NaCl; 6 KCl; 0.33 NaH_2PO_4; 5 sodium pyruvate; 10 glucose; 10 Hepes; 1 $MgCl_2$; 2 $CaCl_2$; pH 7.4. Recordings were made using the whole-cell patch-clamp technique. The pipette solution contained (mM): 140 KCl; 10 Hepes; 1 $MgCl_2$; 5 BAPTA; 5 ATP; 0.1 ADP; pH 7.2. APs were elicited at a frequency of 0.2 Hz under current clamp. APD_{90} values were measured from the upstroke to 90 % repolarisation. pIC_{50} values were determined from plots of percentage increase of APD_{90} against inhibitor concentration. Voltage clamp was used to study the effect of the drugs on I_{Kr} and calcium (I_{Ca}) channels.

The mean control APD_{90} was 439.1 ± 20.1 ms (mean ± S.E.M.; $n = 22$). Dofetilide increased APD_{90} in a concentration-dependent manner; at 1 μM the mean APD_{90} was 854.1 ± 123.1 ms ($n = 5$). The pIC_{50} was 7.3 ± 0.2 ($n = 8$). Dofetilide (1 μM) had no effect on I_{Ca}. Similarly, E-4031 increased APD_{90} in a concentration-dependent manner; pIC_{50} was 7.2 ± 0.02 ($n = 4$). The mean APD_{90} at 1 μM E-4031 was 728.4 ± 41.3 ms ($n = 3$). In contrast, 10 μM cetirizine, inactive at the hERG channel, had little effect on AP duration or Kr channels. Mean APD_{90} values in the absence and presence of the drug were 410.3 ± 48.8 and 455.5 ± 47.1 ms, respectively ($n = 5$).

The potency values measured thus far are comparable to other preparations such as the hERG cell line and Purkinje fibre. The compounds also exhibited similar effects to those observed in telemetry studies on man. In conclusion, these findings warrant further investigation into the possible use of myocytes for screening compounds with potential QT activity.

All procedures accord with current UK legislation.

Protective DNP pretreatment of rat isolated single ventricular myocytes results in production of reactive oxygen species and early activation of sarcolemmal K_{ATP} channels during metabolic inhibition

G.C. Rodrigo, C.L. Lawrence and N.B. Standen

Department of Cell Physiology & Pharmacology, University of Leicester, PO Box 138, Leicester LE1 9HN, UK

Rat ventricular myocytes pretreated with dinitrophenol (DNP) show increased resistance to metabolic inhibition (MI) and reperfusion (Rodrigo *et al.* 2002). We have set out to investigate the possible role of sarcolemmal K_{ATP} channels and their interplay with reactive oxygen species (ROS) in functional recovery of myocytes pretreated with DNP or H_2O_2.

Ventricular myocytes were isolated enzymatically from adult rats killed by cervical dislocation, and loaded with the indicator 6-carboxy 2′,7′-dichlorodihydrocarboxyfluorescein (DCF) to measure H_2O_2 and fura-2 to measure $[Ca^{2+}]_i$. Single channel activity was recorded from cell-attached patch electrodes (140 mM KCl); contractions were monitored with a video system and MI was achieved by superfusion with substrate-free Tyrode solution containing NaCN (2 mM) and iodoacetate (1 mM). Myocytes were pretreated with either 50 μM DNP for 5 min, or 1 μM H_2O_2 for 1 min followed by washing with substrate-free Tyrode solution for 2 min. These cells exhibited increased recovery following MI and reperfusion. 65.2 ± 4.1 % (mean ± S.E.M., $n = 23$; $P < 0.001$ *vs.* control, unpaired *t* test) of DNP-pretreated cells and 47.9 ± 1.4 % ($n = 23$; $P < 0.001$) of H_2O_2-pretreated cells recovered contractile function compared with 19.8 ± 1.9 % ($n = 45$) of control myocytes. Pretreated cells maintained a low resting $[Ca^{2+}]_i$ with a fura-2 ratio (340/380 nm) of 1.65 ± 0.11 ($n = 122$: $P < 0.001$) in DNP-pretreated and 2.35 ± 0.22 ($n = 81$; $P < 0.001$) in H_2O_2-pretreated cells compared with 4.05 ± 0.22 ($n = 275$) in control cells. During MI myocytes pretreated with either DNP or H_2O_2 developed contractile failure earlier than control myocytes at 169 ± 5 s ($n = 40$; $P < 0.001$) and 152 ± 6 s ($n = 48$; $P < 0.001$) respectively compared to 232 ± 6 ($n = 61$) in control cells. DNP pretreatment was also associated with early activation of sarcolemmal K_{ATP} channels in unstimulated myocytes, with the delay to activation significantly reduced from 6.63 ± 0.6 min ($n = 5$: $P < 0.001$) in control myocytes to 2.3 ± 0.5 min ($n = 5$) in DNP-pretreated myocytes. ROS production, determined as the rate of increase in relative DCF fluorescence, was increased from 0.17 ± 0.01 units min^{-1} ($n = 79$) in normal Tyrode solution to 0.73 ± 0.05 ($n = 39$; $P < 0.001$) by 50 μM DNP.

Our results show that pretreatment with DNP or H_2O_2 increases functional recovery of myocytes after MI reperfusion and may be associated with early activation of sarcolemmal K_{ATP} channels during MI. We speculate that an increase in ROS may play a role in early channel activation.

Rodrigo, G.C. *et al.* (2002). *J. Mol. Cell. Cardiol.* **34**, 555–569.

This work was supported by the BHF and The Wellcome Trust.

All procedures accord with current UK legislation.

G-protein-independent inhibition of atrial GIRK current by adenosine in atrial myocytes strongly overexpressing A_1 receptors

L.I. Bösche, A. Rinne, K. Bender, M.-C. Wellner-Kienitz and L. Pott

Institut für Physiologie, Ruhr-Universität Bochum, D-44780 Bochum, Germany

GIRK channels in atrial myocytes are activated by various G-protein-coupled receptors including muscarinic M_2 (M_2AChR) and purinergic A_1 (A_1AdoR). In adult rat atrial myocytes the amplitude of GIRK current evoked by adenosine is limited by the density of A_1AdoR to ~30 % of the current in the presence of ACh at a saturating concentration. Transfection of atrial myocytes with conventional vectors encoding for A_1AdoR increases sensitivity to adenosine (Wellner-Kienitz *et al.* 2000). In the present study we confirmed these results by means of a more efficient adenovirus-based method of gene transfer (He *et al.* 1998). Adult rats were anaesthetized and killed by cervical dislocation. The heart was removed for isolation of myocytes. In a fraction of A_1AdoR transfected myocytes, displaying a particularly high fluorescence-intensity of the reporter protein (GFP), activation of GIRK current by Ado (10 μM) was followed by a rapid decay ($t_{½}$ ~ 300 ms). Upon washout of Ado a rebound of current was observed that was proportional to the degree of the initial decay. In those cells Ado caused an inhibition of M_2AChR-induced current in the continuous presence of ACh. In GTP-γ-S-loaded myocytes stably and irreversibly activated GIRK current was reversibly inhibited by Ado (Fig. 1).

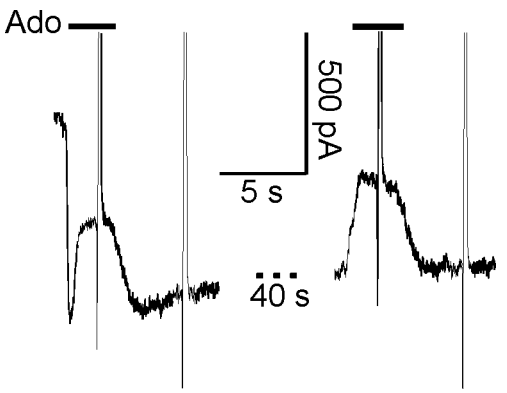

Figure 1. Whole-cell recording from a myocyte transfected with A_1Ado-R adenoviral construct. Recording pipette was supplemented with GTP-γ-S. Ado (10 μM) causes rapid activation followed by transient inhibition of GIRK current. The irreversibly activated current is reversibly inhibited by a second exposure to Ado.

Upon activation of endogenous M_2AChR by a highly saturating concentration of ACh (1 mM), a similar inhibitory component can be detected. These results suggest a novel mechanism of GIRK current inhibition by G-protein-coupled receptors, which requires fast activation of a large number of receptors, and which seems to be independent of GTP cycling of a heterotrimeric G-protein.

He, T.C. *et al.* (1998). *Proc. Natl Acad. Sci. USA* **95**, 2509–2514.
Wellner-Kienitz, M.-C. *et al.* (2000). *Circ. Res.* **86**, 643–648.

This work was supported by Deutsche Forschungsgemeinschaft.

All procedures accord with current National guidelines.

Ca^{2+} modulates I_K, possibly via calmodulin kinase and the SR partially mediates isoprenaline augmentation of I_K

P.A.D. Mattick, B.M. Heath and D.A. Terrar

Oxford University, Oxford, UK

Delayed rectifier potassium currents, rapidly activating I_{Kr} and slowly activating I_{Ks}, play a role in cardiac repolarization, and deactivation of channels carrying these currents contributes to pacemaker activity in the sino-atrial node. Possible influence of cytosolic Ca^{2+} on these currents was investigated in guinea-pig isolated sino-atrial (SA) node cells.

SA node cells were isolated from hearts removed from guinea-pigs following stunning and cervical dislocation. Cells were superfused with a physiological salt solution containing 2.5 mM Ca^{2+} at 36 °C. Cells were voltage-clamped using a perforated-patch clamp technique. All currents were activated from a holding potential of −40 mV, I_K was measured using tail currents, and values stated as a mean ± S.E.M. % of the maximum control current at 700 ms. Under these conditions, currents after 40 ms depolarisations reflect predominantly I_{Kr}, while I_{Ks} contributes substantially to currents after 700 ms depolarisations. Statistical significance was evaluated using Student's paired *t* test.

BAPTA (10 μM) suppressed I_K at both 40 ms (7 ± 2 *vs.* 23 ± 5 %; $P < 0.05$; $n = 6$) and 700 ms (28 ± 5 *vs.* 100 ± %; $P < 0.05$; $n = 6$) duration depolarisations (to 40 mV). Nifedipine (5 μM) reduced I_K amplitude at both 40 ms (12 ± 1 *vs.* 17 ± 2 %; $P < 0.05$; $n = 11$) and 700 ms (85 ± 5 *vs.* 100 ± 0 %; $P < 0.05$; $n = 11$). Ryanodine (5 μM) also reduced I_K, but only after long duration depolarisations: 700 ms (82 ± 7 *vs.* 100 ± 0 %; $P < 0.05$; $n = 9$). KN93 (an inhibitor of calmodulin-dependent kinase) reduced current at 40 ms from 27 to 12 % and at 700 ms from 100 to 45 %. Isoprenaline (100 nM) increased I_K amplitude from 22 ± 6 to 37 ± 7 % at 40 ms ($P < 0.05$; $n = 9$) and 100 ± 0 to 197 ± 16 % at 700 ms ($P < 0.05$; $n = 9$); however, when SR Ca^{2+} release was inhibited with ryanodine, isoprenaline only increased the I_K amplitude of the longer duration depolarisation: 100 ± 0 to 132 ± 8 % at 700 ms ($P < 0.05$; $n = 5$).

These observations are consistent with an influence of cytsolic Ca^{2+} on delayed rectifier potassium currents. Buffering Ca^{2+} with BAPTA appeared to influence both components, as did blocking Ca^{2+} entry with nifedipine. Block of ryanodine-sensitive release channels in the SR appeared to affect predominantly I_{Ks}. Isoprenaline actions on I_K appear to be influenced by SR Ca^{2+}. These actions might be in part be mediated through a kinase mechanism since the inhibitor KN-93 appeared to reduce both I_{Kr} and I_{Ks}, though further experiments are needed to test these possibilities.

This work was funded by the British Heart Foundation.

All procedures accord with current UK legislation.

Caffeine partially inhibits transient outward (I_{to}) and delayed rectifier (I_K) potassium currents in isolated rat ventricular myocytes

Alzbeta Chorvatova and Munir Hussain

Department of Medicine, University of Liverpool, Daulby Street, Liverpool L69 3GA, UK

High concentrations of caffeine are known to inhibit inward rectifier (I_{K1}) potassium currents (Varro *et al.* 1993; Cui & Terrar, 1995). In the present study we investigated whether caffeine also inhibted I_{to} and I_K.

Rats were stunned and humanely killed by cervical dislocation (Schedule 1, Scientific Procedures Act, 1986). The heart was digested with collagenase and protease to isolate ventricular myocytes. Voltage clamp was performed using the perforated patch method using amphotericin B (240 μg ml^{-1}). Internal pipette solutions contained (mmol l^{-1}): potassium glutamate, 120; KCl, 20; NaCl, 10 and Hepes, 10; pH 7.25 with KOH. External solutions contained (mmol l^{-1}): NaCl, 140; KCl, 5.4; $MgCl_2$, 1; $CaCl_2$, 1; glucose, 10; Hepes, 10; pH 7.35 with NaOH. Experiments were carried out at 35 °C. Data are presented as means ± S.E.M.

Initial experiments verified the inhibitory action of 10 mmol l^{-1} caffeine on I_{K1}, and showed that these effects were independent of $[Ca^{2+}]_i$, as described previously (Cui & Terrar, 1995). Simultaneous measurement of sacolemmal current and $[Ca^{2+}]_i$ with fura-2 showed that inhibition of the outward component of I_{K1} could account for the inhibitory effect of caffeine on the background holding current observed at −40 mV: the holding current was inhibited by 0.53 ± 0.10 pA pF^{-1} ($n = 4$) in the absence and by 0.48 ± 0.20 pA pF^{-1} ($n = 4$) in the presence of 10 μmol l^{-1} BAPTA.

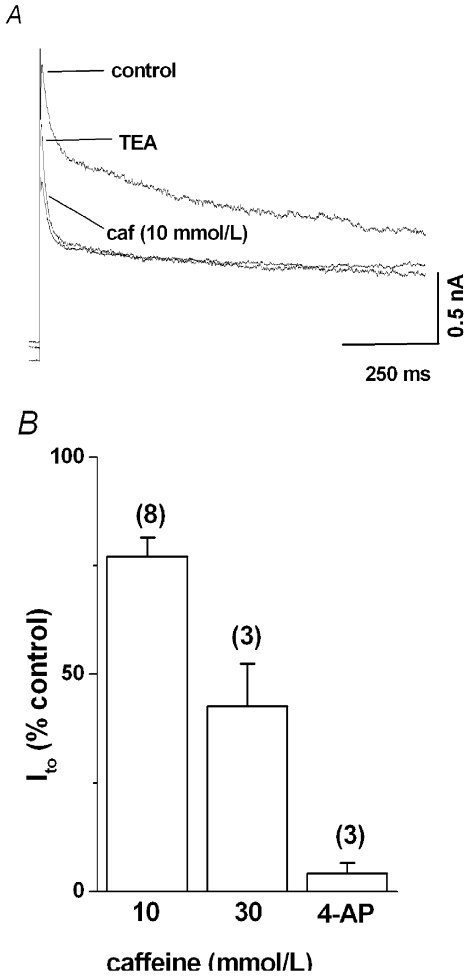

Figure 1. Effect of caffeine and TEA on I_K and I_{to} (*A*) in isolated rat ventricular myocytes.Effect of caffeine and 4-AP on I_{to} (*B*).

I_{to}, elicited by square voltage pulses of 1 s duration from −40 to +60 mV, was inhibited by 1.75 ± 0.52 pA pF^{-1} (n = 4) in the presence of 10 mmol l^{-1} caffeine, without altering the voltage dependence of activation or inactivation. Steady-state I_K, recorded at the end of clamp pulse, were inhibited by 2.15 ± 0.25 pA pF^{-1} (n = 7) in the presence of 10 mmol l^{-1} caffeine (Fig. 1). These data show that caffeine has a small but significant inhibitory action on three different types of K channels in cardiac muscle.

Cui, Y. & Terrar, D.A. (1995). *J. Cardiovasc. Pharmacol.* **25**, 691–695.
Varro, A. et al. (1993). *Br. J. Pharmacol.* **109**, 895–897.

All procedures accord with current UK legislation.

Heterogeneity of outward K$^+$ currents in isolated rat ventricular myocytes: contribution of the novel component, I_{Kx}

Andrew F. James*†, Stephanie C.M. Choisy*, Judith E. Ramsey† and A. Martyn Reynolds†

**Department of Physiology & Cardiovascular Research Laboratories, School of Medical Sciences, University of Bristol, University Walk, Bristol BS8 1TD and †Cardiac Physiology, St Thomas' Hospital, King's College London, London SE1 7EH, UK*

A novel component to the outward currents of rat ventricular myocytes, I_{Kx}, has recently been suggested (Himmel *et al.* 1999). We have investigated the contribution of I_{Kx} to the outward currents recorded from 103 rat ventricular myocytes at physiological temperatures and in the absence of external Cd^{2+} using conventional whole-cell patch-clamp techniques. Left ventricular myocytes were isolated enzymatically from hearts excised under pentobarbitone anaesthesia (150 mg kg^{-1} I.P.) from adult male Wistar rats according to UK legislation. Isolated cells were superfused with a Hepes-buffered Tyrode solution containing 1 mM Ca^{2+} (pH 7.35) at 35 °C. Pipettes were filled with a Hepes-buffered K^+-rich solution containing 10 mM EGTA and 4 mM ATP (pH 7.2, pCa 7.14). Na^+ and Ca^{2+} currents were removed using 20 ms pre-pulses to −40 mV and 3 μM nifedipine, respectively. Data are given as means ± S.E.M. and $P < 0.05$ in a Student's paired t test was considered statistically significant. The voltage-dependent inactivation of the currents was examined using a two-pulse protocol in which 1 s conditioning pulses from −100 to +5 mV were given immediately prior to a 1 s pulse to +40 mV. Modified Boltzmann equations comprising either a single or two inactivating components were fitted by non-linear least squares to the inactivation of the peak current (I_{pk}) from conditioning pulses positive to −80 mV. In 81 of the myocytes examined, a modified Boltzmann equation with two inactivating components was accepted as a good fit to the data:

$$I_{pk} = I_{m1}/(1 + \exp((V_p - V_{0.5,1})/V_{s,1})) + I_{m2}/(1 + \exp((V_p - V_{0.5,2})/V_{s,2})) + I_{ss},$$

where I_{m1} and I_{m2} are the maximal values of the inactivating components, I_{ss} is the non-inactivating component, V_p is the conditioning pulse potential, $V_{0.5,1}$, $V_{0.5,2}$, $V_{s,1}$ and $V_{s,2}$ are the voltages of half-maximal inactivation and slope factors of the respective current components. The mean values of $V_{0.5,1}$ (−50.5 ± 0.5 mV) and $V_{0.5,2}$ (−29.5 ± 0.7 mV, n = 81, $P < 0.001$) are consistent with the existence of I_{to1} and I_{Kx}, respectively. In paired t tests, the mean of I_{Kx} (352 ± 24 pA) was significantly less than that of I_{to1} (734 ± 59 pA; $P < 0.001$) or I_{ss} (644 ± 28 pA; $P < 0.001$). However, there was considerable heterogeneity between cells, the relative contribution of I_{Kx} ranging from 2.5 to 51 % of the total peak outward current. Thus I_{Kx} is likely to play an important role in the heterogeneity of repolarising K^+ currents in rat ventricular myocytes.

Himmel, H.M. *et al.* (1999). *Am. J. Physiol.* **277**, H107–118.

Financial support from The Wellcome Trust and British Heart Foundation is gratefully acknowledged.

All procedures accord with current UK legislation.

Modelling cross-talk of mechano-dependent Ca^{2+} handling and stretch-activated currents in cardiac mechanoelectric feedback

Nathalie Vikulova, Olga Solovyova, Vladimir Markhasin and Peter Kohl*

*Ekaterinburg Branch of the Institute of Ecology and Genetics of Microorganisms, Pervomayskaya 91, Ekaterinburg, Russia and *University Laboratory of Physiology, Parks Road, Oxford OX1 3PT, UK*

Experimental findings on mechanoelectric feedback in isolated myocardium and single cardiomyocytes have yielded a wide variety of stretch-induced changes in action potential duration (APD).

Earlier mathematical modelling has shown that APD responses may depend on stretch timing and the predominant mechano-sensitive mechanism activated. Thus early activation of stretch-activated ion channels (SACs) shortens APD, while late activation prolongs it. The opposite effects may be observed if the predominant target mechanism is troponin C (TnC) affinity for Ca^{2+} (Kohl *et al.* 1998).

To extend applicability of the model to contraction-related mechanical modulation of cardiomyocyte electrophysiology during various modes of contraction, we developed the Ekaterinburg/Oxford model which uses an improved description of cellular Ca^{2+} handling and mechanics, namely co-operative modulation of Ca^{2+} dissociation from TnC (Garny *et al.* 2001). This allowed us to relate changes in APD to length-dependent differences in Ca^{2+} dissociation from TnC and knock-on effects on Ca^{2+} transient and Na^{+}–Ca^{2+} exchange current (i_{NaCa}). The model simulated a range of stretch effects, but not cross-over of repolarisation and late APD prolongation, or after-depolarisation-like events during large stretch. Only then did the model produce these effects when we also included SAC currents (i_{SAC}).

We developed a routine that allows quantitative assessment of the influence of stretch-induced change in individual currents on AP shape. This is based on calculation of the cumulative effect (integral) of the difference Δi_k in the kth current during mechanical stimulation and control. The integrals contribute to AP change as in:

$$\Delta E(t) = E_{\text{stretch}}(t) - E_{\text{control}}(t) = \Delta E(t_0) - \frac{1}{C}\sum_{k=1}^{n}\int_{t_0}^{t}\Delta i_k(\tau)d\tau.$$

Comparison of integrals allows elucidation of the relative significance of individual currents for observed total AP change. Thus in the case of a small SAC conductance (0.03 nS for both control sarcomere length 1.9 μm and 5% stretch), stretch-induced APD shortening is caused by a repolarising effect on AP of change in both i_{NaCa} and i_{SAC} (Fig. 1*A*). In the case of high SAC conductance (0.66 nS for 5% stretch), the cross-over of repolarisation is driven by the opposite effects of these current changes (Fig. 1*B*).

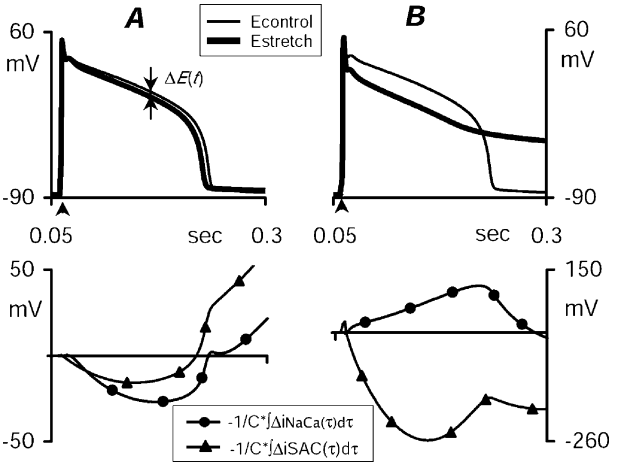

Figure 1. Cumulative effects of stretch-induced changes in i_{NaCa} and i_{SAC} on AP. *A*, small SAC conductance; *B*, high SAC conductance. Top: membrane potential. Bottom: difference current integrals.

Garny, A.F. *et al.* (2001). *XXXIV IUPS Congress,* Abstract, CD, Christchurch, NZ, a83.pdf.

Kohl, P. *et al.* (1998). *Can. J. Cardiol.* **14**, 111–119.

This work is supported by The Wellcome Trust and the Russian Foundation for Basic Research.

Compression activates and stretch deactivates non-selective cation currents in isolated rat atrial fibroblasts

A. Kamkin*, I. Kiseleva* and G. Isenberg†

**Institute of Physiology* (*Charité*), *Tucholskystr. 2, 10117 Berlin, Germany and †Department of Physiology, Martin Luther University, Magdeburgerstrasse 6, D-06097, Halle, Germany*

Fibroblasts are the most numerous non-myocyte cells of the heart (Eghbali *et al.* 1988). They constitute a volume fraction that is 5–10% of the heart cell volume (Anversa *et al.* 1980) and up to 75% in the sinus node (Shiraishi *et al.* 1992). Microelectrode recordings from rat atrial multicellular tissue indicate that fibroblasts have resting potentials (E_0) between −5 and −70 mV and input resistances (R_{in}) between 0.4 and 0.6 GΩ (Kiseleva *et al.* 1998). The fibroblast membrane potential is modulated by mechanical stretch and pressure (Kiseleva *et al.* 1998), a property that may contribute to the intracardiac mechanoelectrical feedback (Kamkin *et al.* 2002). It was supposed that compression of fibroblasts during contraction of the tissue leads to depolarization and stretch leads to hyperpolarisation. We tested this hypothesis and studied the nature of these effects.

Fibroblasts, which were isolated from rat hearts excised under ether anaesthesia were used for a voltage-clamp. The fibroblast was mechanically deformed between two patch pipettes, the first pipette was used for whole-cell clamp and served as a fix point. The second cell-attached pipette was laterally displaced with regard to the first pipette, thereby compressing or stretching the cell. The dependence of ionic current on membrane potential (*I–V* relationship) was measured by applying 20 pulses of 140 ms

(0.5 Hz) that started from a holding potential of −45 mV. When the membrane currents flowing at the end of the pulse (I_L) were plotted *versus* the respective clamp step potential, the resulting *I–V* curve intersected the voltage axis at the zero current potential (E_0, corresponding to the resting potential of non-clamped cells). On average, the isolated fibroblast had an $E_0 = -37 \pm 3$ mV ($n = 50$), and the $R_{in} = 514 \pm 11$ MΩ ($n = 50$) that resembled their counterparts in multicellular strips. Compression by 2, 3, or 4 μm shifted E_0 to depolarization (Fig. 1, Table 1). The compression-induced difference (I_{ci}) followed a modest outward rectification. Their amplitude increased with the extent of compression (Table 1) whilst their reversal potential (E_{rev}) was nearly constant. The currents were carried by Na^+, K^+ and Cs^+ ions, and were blocked by extracellular application of 8 μM Gd^{3+}. The results suggest that compression induces a non-selective cation conductance (G_{ns}). Stretch by 2, 3 or 4 μm hyperpolarized E_0 (Fig. 1, Table 2). Stretch induced a positive difference current (I_{str}) with a E_{rev} close to 0 mV (Table 2). Application of Gd^{3+} during continuous stretch shifted E_0 to potentials as negative to E_K (−97 ± 5 mV).

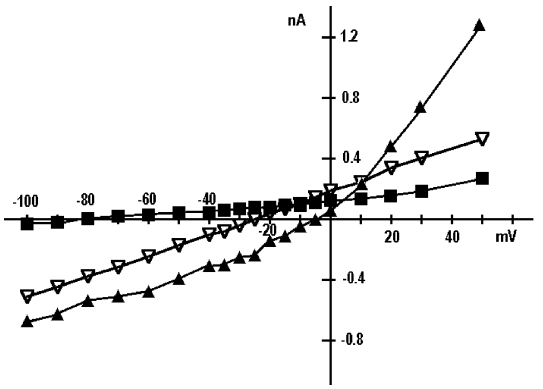

Figure 1. Compression of the cell increases and stretch of the cell decreases net membrane currents. Current–voltage relationship of the currents measured at the end of the pulse (late current I_L). Open triangles, before the mechanical stress; filled trianlges, compression by 3 μm; filled squares, stretch by 3 μm.

Table 1
Compression induced changes in the electrical parameters of fibroblasts.

n	4	4	5
ΔL (μm)	2	3	4
R (MΩ) C (pF)	588±76 18±2	577±80 19±2	539±96 18±2
E_0 (mV)	-34±5	-35±5	-33±6
$E_{0,\Delta L}$ (mV) I_{ci} at −45 mV (nA) E_{rev} (mV)	-24±3 -0.03±0.01 +5±3	-10±3 -0.18±0.05** +11±2	-5±2 -0.34±0.09$^{+++\dagger\dagger}$ +16±3
$I_{ci,Gd}$ at −45 mV (nA)	0.04±0.02	0.24±0.05**	0.38±0.08$^{+++\dagger\dagger}$
$E_{0,\Delta L,Gd}$ (mV)	-87±6	-80±5	-85±6

Compression of the cell: *3 μm vs. 2 μm: ** P<0.01, *** P<0.001; ANOVA
$^+$ 4 μm vs. 2 μm $^{+++}$ P<0.001; † 4 μm vs. 3 μm, † P<0.05, †† P<0.01;

Table. 2
Stretch induced changes in the electrical parameters of fibroblasts.

ΔL (μm)	2	3	4
n	4	4	4
R (MΩ) C (pF)	501±57 18±2	547±85 16±2	585±48 18±2
E_0 (mV)	-35±6	-35±5	-33±3
$E_{0,\Delta L}$ (mV) I_{str} at −45 mV (nA) E_{rev} (mV)	-43±6 0.05±0.02 0±2	-52±3 0.12±0.04*** - 6±1	-82±8 0.37±0.03$^{+++\dagger\dagger\dagger}$ -10±2
$I_{str,Gd}$ at −45 mV (nA)	0.07±0.02	0.15±0.03***	0.55±0.12$^{+++\dagger\dagger\dagger}$
$E_{0,\Delta L,Gd}$ (mV)	-97±5	-98±4	-95±4

Stretch of the cell: * 3 μm vs. 2 μm *** P<0.001; ANOVA
$^+$ 4 μm vs. 2 μm $^{+++}$ P<0.001; † 4 μm vs. 3 μm ††† P<0.001

Ion selectivity, E_{rev} and Gd^{3+} sensitivity of stretch-suppressed currents let us suggest that stretch reduces G_{ns}. Cell dialysis with BAPTA (pCa > 8) or Ca^{2+}/EGTA (pCa = 6) or with EGTA (pCa = 7) had no influence on the I_{ci} or I_{str}, suggesting that Ca^{2+}-dependent conductances are unlikely to contribute. The results could be modelled on the assumption of a compression-induced, stretch-deactivated G_{ns} operating in parallel with a mechano-insensitive K^+ conductance and a current due to electrogenic Na^+ pumping.

Anversa, P. *et al.* (1980). *J. Mol. Cell Cardiol.* **12**, 781–795.
Eghbali, M. *et al.* (1988). *J. Mol. Cell Cardiol.* **20**, 267–276.
Kamkin, A. *et al.* (2002). *Am. J. Physiol.* **282**, H842–849.
Kiseleva, I. *et al.* (1998). *J. Mol. Cell Cardiol.* **30**, 1083–1093.
Shiraishi, I. *et al.* (1992). *Circulation* **85**, 2176–2184.

All procedures accord with current National guidelines.